

# The voltage-gated channels of $\text{Na}^+$ action potentials

The ionic basis for nerve excitation was first elucidated in the squid giant axon by Hodgkin and Huxley (1952) using the voltage clamp technique. They made the key observation that two separate, voltage-dependent currents underlie the action potential: an early transient inward  $\text{Na}^+$  current which depolarizes the membrane, and a delayed outward  $\text{K}^+$  current largely responsible for repolarization. This led to a series of experiments that resulted in a quantitative description of impulse generation and propagation in the squid axon.

Nearly 30 years later, Sakmann and Neher, using the patch clamp technique, recorded the activity of the voltage-gated  $\text{Na}^+$  and  $\text{K}^+$  channels responsible for action potential initiation and propagation. Taking history backwards, action potentials will be explained from the single channel level to the membrane level.

## 4.1 PROPERTIES OF ACTION POTENTIALS

### 4.1.1 The different types of action potentials

The action potential is a sudden and transient depolarization of the membrane. The cells that initiate action potentials are called 'excitable cells'. Action potentials can have different shapes, i.e. different amplitudes and durations. In neuronal somas and axons, action potentials have a large amplitude and a small duration: these are the  $\text{Na}^+$ -dependent action potentials (**Figures 4.1** and **4.2a**). In other neuronal cell bodies, heart ventricular cells and axon terminals, the action potentials have a longer duration with a plateau following the initial peak: these are the  $\text{Na}^+/\text{Ca}^{2+}$ -dependent action potentials

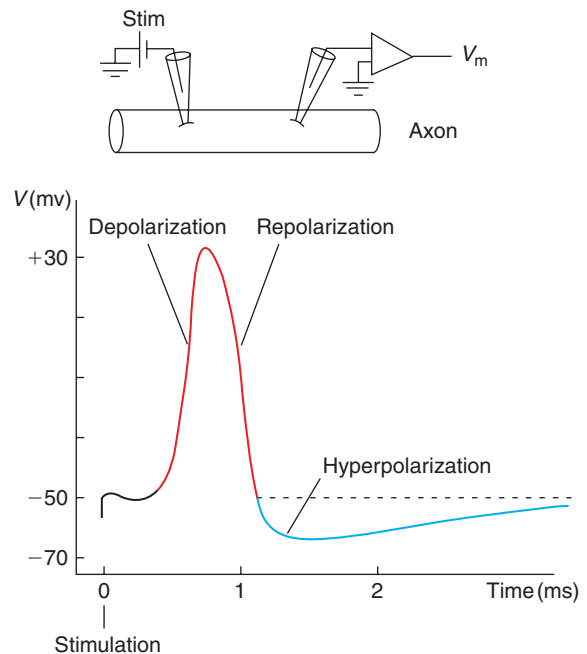


**FIGURE 4.1** Action potential of the giant axon of the squid.

Action potential intracellularly recorded in the giant axon of the squid at resting membrane potential in response to a depolarizing current pulse (the extracellular solution is seawater). The different phases of the action potential are indicated. Adapted from Hodgkin AL and Katz B (1949) The effect of sodium ions on the electrical activity of the giant axon of the squid. *J. Physiol.* **108**, 37–77, with permission.

(**Figure 4.2b-d**). Finally, in some neuronal dendrites and some endocrine cells, action potentials have a small amplitude and a long duration: these are the  $\text{Ca}^{2+}$ -dependent action potentials.

Action potentials have common properties; for example they are all initiated in response to a membrane

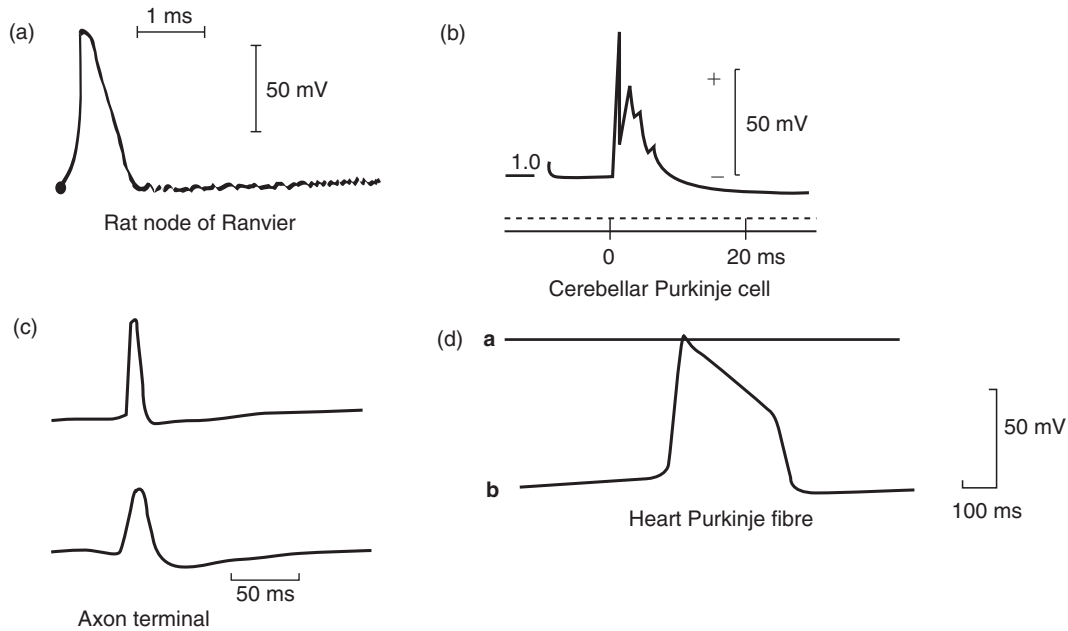


**FIGURE 4.2** Different types of action potentials recorded in excitable cells.

(a) Sodium-dependent action potential intracellularly recorded in a node of Ranvier of a rat nerve fibre. Note the absence of the hyperpolarization phase following the action potential. (b)–(d) Sodium–calcium-dependent action potentials. Intracellular recording of the complex spike in a cerebellar Purkinje cell in response to climbing fibre stimulation: an initial  $\text{Na}^+$ -dependent action potential and a later larger slow potential on which are superimposed several small  $\text{Ca}^{2+}$ -dependent action potentials. The total duration of this complex spike is 5–7 ms. (b) Action potential recorded from axon terminals of *Xenopus* hypothalamic neurons (these axon terminals are located in the neurohypophysis) in control conditions (top) and after adding blockers of  $\text{Na}^+$  and  $\text{K}^+$  channels (TTX and TEA, bottom) in order to unmask the  $\text{Ca}^{2+}$  component of the spike (this component has a larger duration due to the blockade of some of the  $\text{K}^+$  channels). (c) Intracellular recording of an action potential from an acutely dissociated dog heart cell (Purkinje fibre). Trace 'a' is recorded when the electrode is outside the cell and represents the trace 0 mV. Trace 'b' is recorded when the electrode is inside the cell. The peak amplitude of the action potential is 75 mV and the total duration 400 ms. (d) All these action potentials are recorded in response to an intracellular depolarizing pulse or to the stimulation of afferents. Note the differences in their durations. Part (a) adapted from Brismar T (1980) Potential clamp analysis of membrane currents in rat myelinated nerve fibres. *J. Physiol.* **298**, 171–184, with permission. Parts (b)–(d) adapted from Coraboeuf E and Weidmann S (1949) Potentiel de repos et potentiels d'action du muscle cardiaque, mesurés à l'aide d'électrodes internes. *C. R. Soc. Biol.* **143**, 1329–1331; and Eccles JC, Llinas R, Sasaki K (1966) The excitatory synaptic action of climbing fibres on the Purkinje cells of the cerebellum. *J. Physiol.* **182**, 268–296; and Obaid AL, Flores R, Salzberg BM (1989) Calcium channels that are required for secretion from intact nerve terminals of vertebrates are sensitive to  $\omega$ -conotoxin and relatively insensitive to dihydropyridines. *J. Gen. Physiol.* **93**, 715–730; with permission.

depolarization. They also have differences; for example in the type of ions involved, their amplitude, duration, etc.

#### 4.1.2 $\text{Na}^+$ and $\text{K}^+$ ions participate in the action potential of axons

The activity of the giant axon of the squid is recorded with an intracellular electrode (in current clamp; see **Appendix 4.1**) in the presence of seawater as the external solution.

*$\text{Na}^+$  ions participate in the depolarization phase of the action potential*

When the extracellular solution is changed from seawater to a  $\text{Na}^+$ -free solution, the amplitude and

risetime of the depolarization phase of the action potential gradually and rapidly decreases, until after 8 s the current pulse can no longer evoke an action potential (**Figure 4.3**). Moreover, in control seawater, tetrodotoxin (TTX), a specific blocker of voltage-gated  $\text{Na}^+$  channels, completely blocks action potential initiation (**Figure 4.4a,c**), thus confirming a major role of  $\text{Na}^+$  ions.

*$\text{K}^+$  ions participate in the repolarization phase of the action potential*

Application of tetraethylammonium chloride (TEA), a blocker of  $\text{K}^+$  channels, greatly prolongs the duration of the action potential of the squid giant axon without

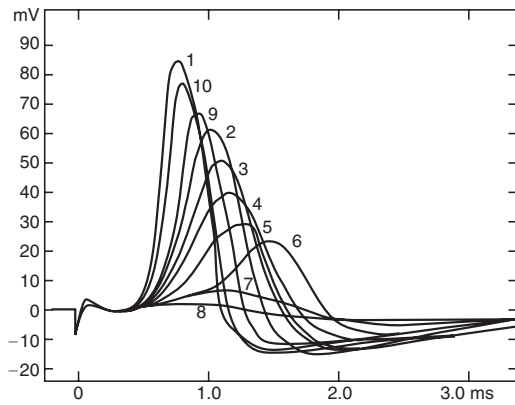


**FIGURE 4.3** The action potential of the squid giant axon is abolished in a Na<sup>+</sup>-free external solution.

(1) Control action potential recorded in sea water; (2)–(8) recordings taken at the following times after the application of a dextrose solution (Na-free solution): 2.30, 4.62, 5.86, 6.10, 7.10 and 8.11 s; (9) recording taken 9 s after reapplication of seawater; (10) recording taken at 90 and 150 s after reapplication of seawater; traces are superimposed. From Hodgkin AL and Katz B (1949) The effect of sodium ions on the electrical activity of the giant axon of the squid. *J. Physiol.* **108**, 37–77, with permission.

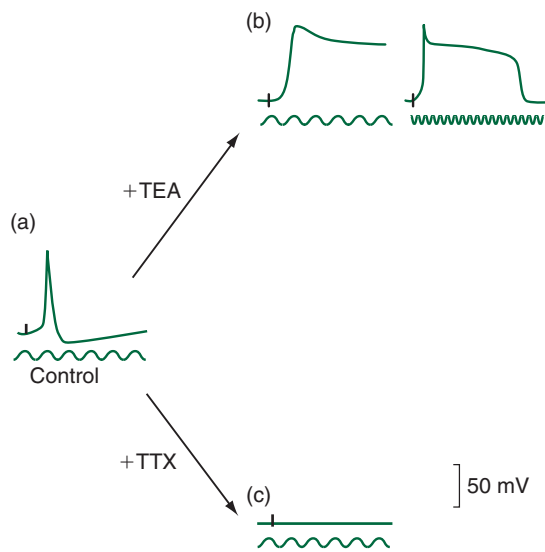


**FIGURE 4.4** Effects of tetrodotoxin (TTX) and tetraethylammonium chloride (TEA) on the action potential of the squid giant axon. (a) Control action potential. (b) TEA application lengthens the action potential (left), which then has to be observed on a different time scale (right trace). (c) TTX totally abolishes the initiation of the action potential. Adapted from Tasaki I and Hagiwara S (1957) Demonstration of two stable potential states in the squid giant axon under tetraethylammonium chloride. *J. Gen. Physiol.* **40**, 859–885, with permission.

changing the resting membrane potential. The action potential treated with TEA has an initial peak followed by a plateau (**Figure 4.4a,b**) and the prolongation is sometimes 100-fold or more.

### 4.1.3 Na<sup>+</sup>-dependent action potentials are all or none and propagate along the axon with the same amplitude

Depolarizing current pulses are applied through the intracellular recording electrode, at the level of a neuronal soma or axon. We observe that (i) to a certain level of membrane depolarization called the threshold potential, only an ohmic passive response is recorded (**Figure 4.5a**, right); (ii) when the membrane is depolarized just above threshold, an action potential is recorded. Then, increasing the intensity of the stimulating current pulse does not increase the amplitude of the action potential (**Figure 4.5a**, left). The action potential is all or none.

Once initiated, the action potential propagates along the axon with a speed varying from 1 to 100 m s<sup>-1</sup> according to the type of axon. Intracellular recordings at varying distances from the soma show that the amplitude of the action potential does not attenuate: the action potential propagates without decrement (**Figure 4.5b**).

### 4.1.4 Questions about the Na<sup>+</sup>-dependent action potential

- What are the structural and functional properties of the Na<sup>+</sup> and K<sup>+</sup> channels of the action potential? (Sections 4.2 and 4.3)
- What represents the threshold potential for action potential initiation? (Section 4.4)
- Why is the action potential, all or none? (Section 4.4)
- What are the mechanisms of action potential propagation? (Section 4.4)

## 4.2 THE DEPOLARIZATION PHASE OF Na<sup>+</sup>-DEPENDENT ACTION POTENTIALS RESULTS FROM THE TRANSIENT ENTRY OF Na<sup>+</sup> IONS THROUGH VOLTAGE-GATED Na<sup>+</sup> CHANNELS

### 4.2.1 The Na<sup>+</sup> channel consists of a principal large $\alpha$ -subunit with four internal homologous repeats and auxiliary $\beta$ -subunits

The primary structures of the *Electrophorus* electroplax Na<sup>+</sup> channel, that of the rat brain, heart and skeletal muscles have been elucidated by cloning and sequence analysis of the complementary cDNAs. The Na<sup>+</sup> channel in all these structures consists of an  $\alpha$ -subunit of approximately 2000 amino acids (260 kDa),

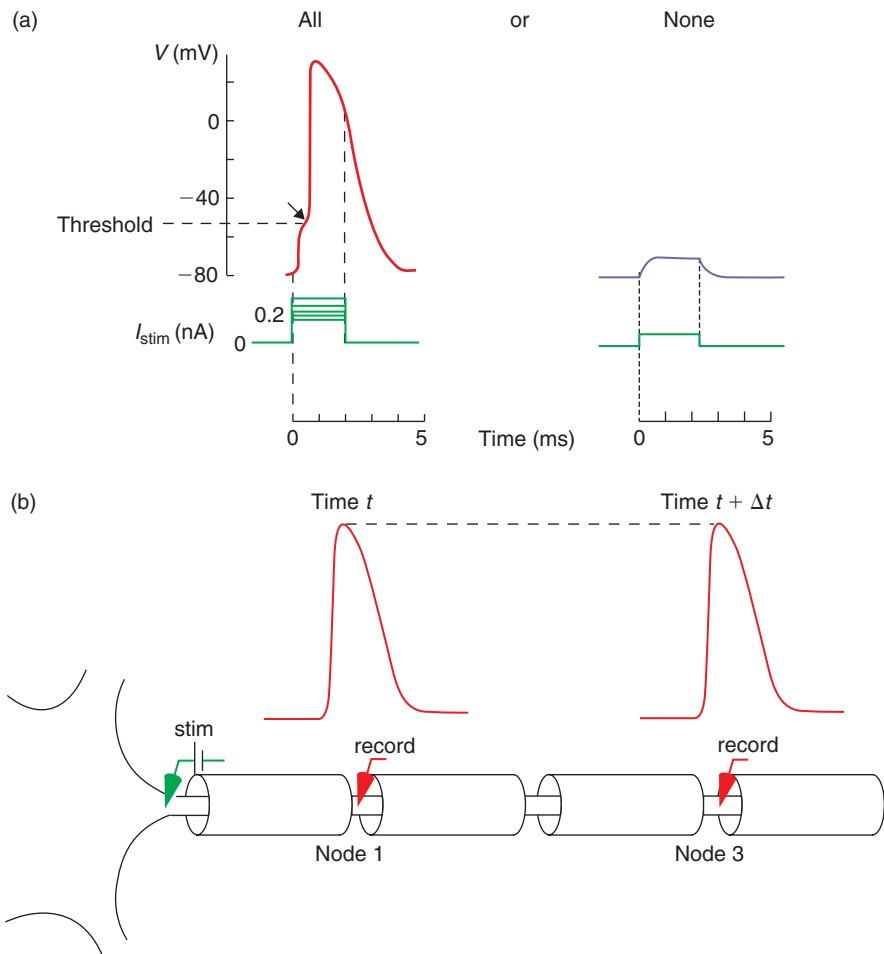


**FIGURE 4.5** Properties of the  $\text{Na}^+$ -dependent action potential.

The response of the membrane to depolarizing current pulses of different amplitudes is recorded with an intracellular electrode. Upper traces are the voltage traces, bottom traces are the current traces. Above 0.2 nA an axon potential is initiated. Increasing the current pulse amplitude does not increase the action potential amplitude (left). With current pulses of smaller amplitudes, no action potential is initiated. **(b)** An action potential is initiated in the soma–initial segment by a depolarizing current pulse (stim). Intracellular recording electrodes inserted along the axon record the action potential at successive nodes at successive times. See text for further explanations.

composed of four homologous domains (I to IV) separated by surface loops of different lengths. Within each domain there are six segments forming six putative transmembrane  $\alpha$ -helices (S1 to S6) and a hairpin-like P loop also called re-entrant pore loop between S5 and S6 (**Figure 4.6a**). The four homologous domains probably form a pseudo-tetrameric structure whose central part is the permeation pathway (**Figure 4.6b**). Parts of the  $\alpha$ -subunit contributing to pore formation have been identified by site-directed mutagenesis.

Each domain contains a unique segment, the S4 segment, with positively charged residues (arginine or lysine) at every third position with mostly non-polar residues intervening between them (see **Figure 4.15a**). This structure of the S4 segment is strikingly conserved in all the types of  $\text{Na}^+$  channels analyzed so far and

this led to suggestions that the S4 segments serve as voltage sensors (see Section 4.2.7).

The  $\alpha$ -subunit of mammals is associated with one or two smaller auxiliary subunits named  $\beta$ -subunits. They are small proteins of about 200 amino acid residues (33–36 kDa), with a substantial N-terminal domain, a single putative membrane spanning segment and a C-terminal intracellular domain.

The  $\alpha$ -subunit mRNA isolated from rat brain or the  $\alpha$ -subunit RNAs transcribed from cloned cDNAs from a rat brain are sufficient to direct the synthesis of functional  $\text{Na}^+$  channels when injected into oocytes. These results establish that the protein structures necessary for voltage-gating and ion conductance are contained within the  $\alpha$ -subunit itself. However, the properties of these channels are not identical to native  $\text{Na}^+$  channels

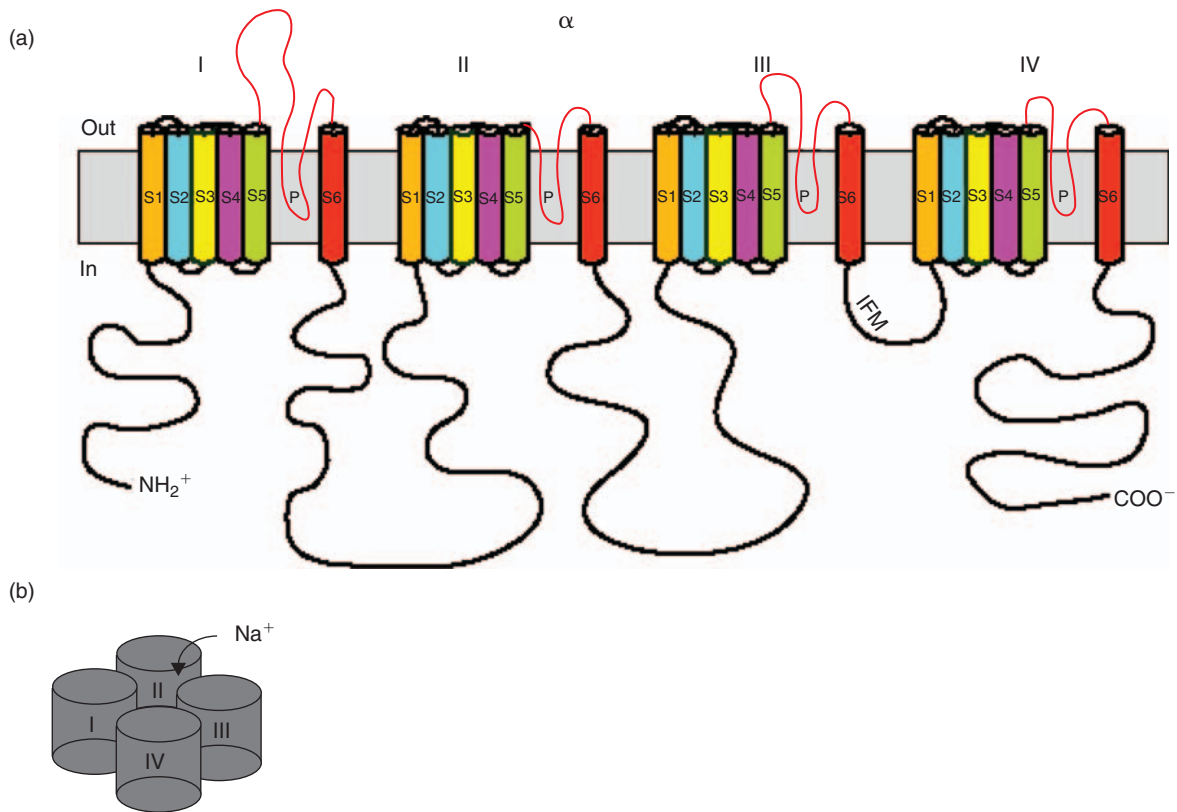


**FIGURE 4.6** A schematic drawing of the voltage-gated Na<sup>+</sup> channel  $\alpha$ -subunit.

(a) Cylinders represent putative membrane-spanning segments, P the P loops and IFM the critical motif of the fast inactivation particle on the cytoplasmic linker connecting domains III and IV. The lengths that are shown for the N and C termini and the interdomain cytoplasmic loops are consistent with the Na<sub>v</sub>1.2 mammalian Na<sup>+</sup> channel but these linkers (except for that between III and IV) vary greatly in length and sequence among the different Na<sup>+</sup> channel isoforms. (b) Diagram of the pseudo-tetrameric structure whose central part is the permeation pathway. Drawing (a) adapted from Goldin A (2002) The evolution of voltage-gated Na<sup>+</sup> channels. *J. Exp. Biol.* 205, 575–584, with permission.

as it has been shown that the auxiliary  $\beta$ -subunits play a role in the targeting and stabilization of the  $\alpha$ -subunit in the plasma membrane, its sensitivity to voltage and rate of inactivation.

The nomenclature of all Na<sup>+</sup> voltage-gated channels is the following: Na<sub>v</sub> to indicate the principal permeating ion (Na<sup>+</sup>) and the principal physiological regulator (v for voltage), followed by a number that indicates the gene subfamily (currently Na<sub>v</sub>1 is the only subfamily). The number following the decimal point identifies the specific channel isoform (e.g. Na<sub>v</sub>1.1). At present, nine functional isoforms have been identified.

#### 4.2.2 Membrane depolarization favours conformational change of the Na<sup>+</sup> channel towards the open state; the Na<sup>+</sup> channel then quickly inactivates

The function of the Na<sup>+</sup> channel is to transduce *rapidly* membrane depolarization into an entry of Na<sup>+</sup> ions.

The activity of a single Na<sup>+</sup> channel was first recorded by Sigworth and Neher in 1980 from rat muscle cells with the patch clamp technique (cell-attached patch; see Appendix 4.3).

It must be explained that the experimenter does not know, before recording it, which type of channel(s) is in the patch of membrane isolated under the tip of the pipette. He or she can only increase the chance of recording a Na<sup>+</sup> channel, for example, by studying a membrane where this type of channel is frequently expressed and by pharmacologically blocking the other types of channels that could be activated together with the Na<sup>+</sup> channels (voltage-gated K<sup>+</sup> channels are blocked by TEA). The recorded channel is then identified by its voltage dependence, reversal potential, unitary conductance, ionic permeability, mean open time, etc. Finally, the number of Na<sup>+</sup> channels in the patch of membrane cannot be predicted. Even when pipettes with small tips are used, the probability of recording more than one channel can be high because of the type

of membrane patched. For this reason, very few recordings of single native  $\text{Na}^+$  channels have been performed. The number of  $\text{Na}^+$  channels in a patch is estimated from recordings where the membrane is strongly depolarized in order to increase to its maximum the probability of opening the voltage-gated channels present in the patch.

### Voltage-gated $\text{Na}^+$ channels of the skeletal muscle fibre

A series of recordings obtained from a single  $\text{Na}^+$  channel in response to a 40 mV depolarizing step given every second is shown in **Figure 4.7a** and **c**. The holding potential is around  $-70$  mV (remember that in the cell attached configuration, the membrane potential can only be estimated). A physiological extracellular concentration of  $\text{Na}^+$  ions is present in the pipette.

At holding potential, no variations in the current traces are recorded. After the onset of the depolarizing step, unitary  $\text{Na}^+$  currents of varying durations but of the same amplitude are recorded (lines 1, 2, 4, 5, 7 and 8) or not recorded (lines 3, 6 and 9). This means that six times out of nine, the  $\text{Na}^+$  channel has opened in response to membrane depolarization. The  $\text{Na}^+$  current has a rectangular shape and is downward. By convention, inward currents of  $+$  ions (cations) are represented as downward (inward means that  $+$  ions enter the cell; see Section 3.4). The histogram of the  $\text{Na}^+$  current amplitude recorded in response to a 40 mV depolarizing step gives a mean amplitude for  $i_{\text{Na}}$  of around  $-1.6$  pA (see Appendix 4.3).

It is interesting to note that once the channel has opened, there is a low probability that it will reopen during the depolarization period. Moreover, even when the channel does not open at the beginning of the step, the frequency of appearance of  $\text{Na}^+$  currents later in the depolarization is very low; i.e. the  $\text{Na}^+$  channel inactivates.

### Rat brain $\text{Na}^+$ channels

The activity of rat brain  $\text{Na}^+$  channels has been studied in cerebellar Purkinje cells in culture. Each trace of **Figure 4.8a** and **c** shows the unitary  $\text{Na}^+$  currents ( $i_{\text{Na}}$ ) recorded during a 20 ms membrane depolarization to  $-40$  mV (test potential) from a holding potential of  $-90$  mV. Rectangular inward currents occur most frequently at the beginning of the depolarizing step but can also be found at later times (**Figure 4.8a**, line 2). The histogram of the  $\text{Na}^+$  current amplitudes recorded at  $-40$  mV test potential gives a mean amplitude for  $i_{\text{Na}}$  of around  $-2$  pA (**Figure 4.8d**). Events near  $-4$  pA correspond to double openings, meaning that at least two channels are present in the patch.

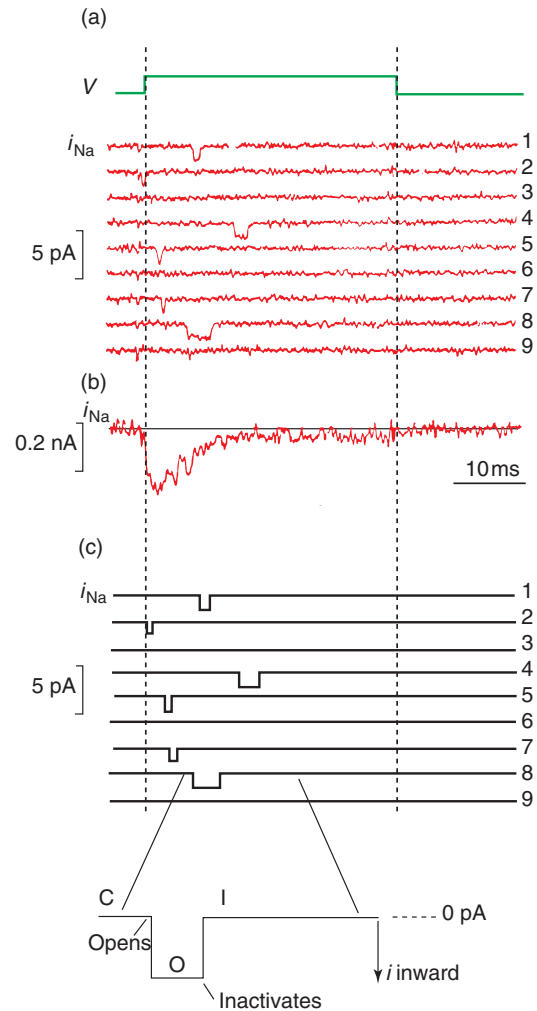
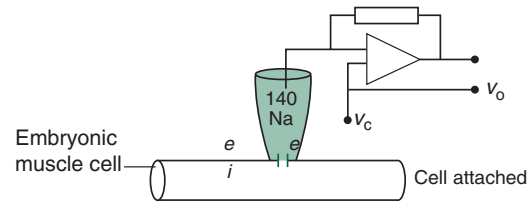


**FIGURE 4.7** Single  $\text{Na}^+$  channel openings in response to a depolarizing step (muscle cell).

The activity of the  $\text{Na}^+$  channel is recorded in patch clamp (cell-attached patch) from an embryonic muscle cell. **(a)** Nine successive recordings of single channel openings ( $i_{\text{Na}}$ ) in response to a 40 mV depolarizing pulse ( $V$  trace) given at 1 s intervals from a holding potential 10 mV more hyperpolarized than the resting membrane potential. **(b)** Averaged inward  $\text{Na}^+$  current from 300 elementary  $\text{Na}^+$  currents as in **(a)**. **(c)** The same recordings as in **(a)** are redrawn in order to explain more clearly the different states of the channel. On the bottom line one opening is enlarged. C, closed state; O, open state; I, inactivated state. The solution bathing the extracellular side of the patch or intrapipette solution contains (in mM): 140 NaCl, 1.4 KCl, 2.0  $\text{MgCl}_2$ , 1  $\text{CaCl}_2$  and 20 HEPES at pH 7.4. TEA 5 mM is added to block  $\text{K}^+$  channels and bungarotoxin to block acetylcholine receptors. Adapted from Sigworth FJ and Neher E (1980) Single  $\text{Na}^+$  channel currents observed in rat muscle cells. *Nature* 287, 447–449, with permission.

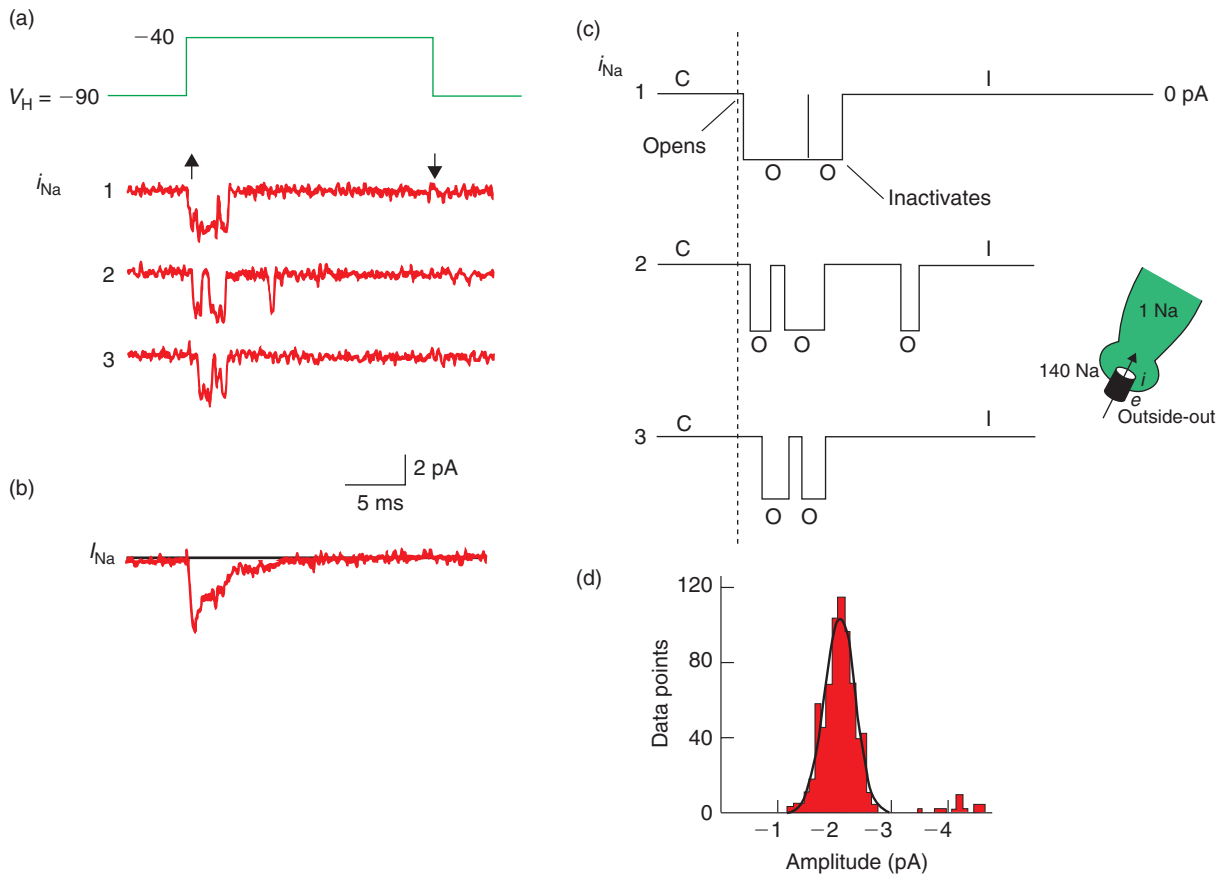


**FIGURE 4.8** Single-channel activity of a voltage-gated  $\text{Na}^+$  channel from rat brain neurons.

The activity of a  $\text{Na}^+$  channel of a cerebellar Purkinje cell in culture is recorded in patch clamp (outside-out patch) in response to successive depolarizing steps to  $-40$  mV from a holding potential  $V_H = -90$  mV. **(a)** The 20 ms step (upper trace) evokes rectangular inward unitary currents ( $i_{\text{Na}}$ ). **(b)** Average current calculated from all the sweeps which had active  $\text{Na}^+$  channels within a set of 25 depolarizations. **(c)** Interpretative drawing on an enlarged scale of the recordings as in **(a)**. The continuous line corresponds to the best fit of the data to a single Gaussian distribution. C, closed state; O, open state; I, inactivated state. The solution bathing the outside face of the patch contains (in mM): 140 NaCl, 2.5 KCl, 1  $\text{CaCl}_2$ , 1  $\text{MgCl}_2$ , 10 HEPES. The solution bathing the inside of the patch or intrapipette solution contains (in mM): 120 CsF, 10 CsCl, 1 NaCl, 10 EGTA- $\text{Cs}^+$ , 10 HEPES- $\text{Cs}^+$ .  $\text{Cs}^+$  ions are in the pipette instead of  $\text{K}^+$  ions in order to block  $\text{K}^+$  channels. Adapted from Gähwiler BH and Llano I (1989) Sodium and potassium conductances in somatic membranes of rat Purkinje cells from organotypic cerebellar cultures. *J. Physiol.* **417**, 105–122, with permission.

### The unitary current has a rectangular shape

The rectangular shape of the unitary current means that when the  $\text{Na}^+$  channel opens, the unitary current is nearly immediately maximal. The unitary current then stays constant: the channel stays open for a time which varies; finally the unitary current goes back to zero though the membrane is still depolarized. The channel may not reopen (**Figure 4.7a,c**) as it is in an inactivated state (I) (**Figure 4.7c**, bottom trace). After being opened by a depolarization, the channel does not go back to the closed state but inactivates. In that state, the pore of the channel is closed (no  $\text{Na}^+$  ions

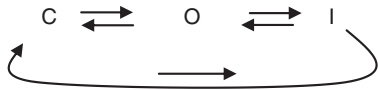
flow through the pore) as in the closed state but the channel cannot reopen immediately (which differs from the closed state). The inactivated channel is refractory to opening unless the membrane repolarizes to allow it to return to the closed (resting) state.

In other recordings, such as that of **Figure 4.8a** and **c**, the  $\text{Na}^+$  channel seems to reopen once or twice before inactivating. This may result from the presence of two (as here) or more channels in the patch so that the unitary currents recorded do not correspond to the same channel. It may also result from a slower inactivation rate of the channel recorded, which in fact opens, closes, reopens and then inactivates.

The unitary current is carried by a few Na<sup>+</sup> ions

How many Na<sup>+</sup> ions enter through a single channel? Knowing that in the preceding example, the unitary Na<sup>+</sup> current has a mean amplitude of  $-1.6 \text{ pA}$  for  $1 \text{ ms}$ , the number of Na<sup>+</sup> ions flowing through one channel during  $1 \text{ ms}$  is  $1.6 \times 10^{-12} / (1.6 \times 10^{-19} \times 10^3) = 10,000$  Na<sup>+</sup> ions (since  $1 \text{ pA} = 1 \text{ pCs}^{-1}$  and the elementary charge of one electron is  $1.6 \times 10^{-19} \text{ C}$ ). This number,  $10^4$  ions, is negligible compared with the number of Na<sup>+</sup> ions in the intracellular medium: if  $[\text{Na}^+]_i = 14 \text{ mM}$ , knowing that 1 mole represents  $6 \times 10^{23}$  ions, the number of Na<sup>+</sup> ions per litre is  $6 \times 10^{23} \times 14 \times 10^{-3} = 10^{22}$  ions  $\text{l}^{-1}$ . In a neuronal cell body or a section of axon, the volume is of the order of  $10^{-12}$  to  $10^{-13}$  litres. Then the number of Na<sup>+</sup> ions is around  $10^9$  to  $10^{10}$ .

The Na<sup>+</sup> channel fluctuates between the closed, open and inactivated states



where C is the channel in the closed state, O in the open state and I in the inactivated state. Both C and I states are non-conducting states. The C to O transition is triggered by membrane depolarization. The O to I transition is due to an intrinsic property of the Na<sup>+</sup> channel. The I to C transition occurs when the membrane repolarizes or is already repolarized. In summary, the Na<sup>+</sup> channel opens when the membrane is depolarized, stays open during a mean open time of less than  $1 \text{ ms}$ , and then usually inactivates.

#### 4.2.3 The time during which the Na<sup>+</sup> channel stays open varies around an average value, $\tau_o$ , called the mean open time

In Figures 4.7a and 4.8a we can observe that the periods during which the channel stays open,  $t_o$ , are variable. The mean open time of the channel,  $\tau_o$ , at a given potential is obtained from the frequency histogram of the different  $t_o$  at this potential. When this distribution can be fitted by a single exponential, its time constant provides the value of  $\tau_o$  (see Appendix 4.3). The functional significance of this value is the following: during a time equal to  $\tau_o$  the channel has a high probability of staying open.

For example, the Na<sup>+</sup> channel of the skeletal muscle fibre stays open during a mean open time of  $0.7 \text{ ms}$ . For the rat brain Na<sup>+</sup> channel of cerebellar Purkinje cells, the distribution of the durations of the unitary currents recorded at  $-32 \text{ mV}$  can be fitted with a single exponential with a time constant of  $0.43 \text{ ms}$  ( $\tau_o = 0.43 \text{ ms}$ ).

#### 4.2.4 The $i_{\text{Na}}-V$ relation is linear: the Na<sup>+</sup> channel has a constant unitary conductance $\gamma_{\text{Na}}$

When the activity of a single Na<sup>+</sup> channel is now recorded at different test potentials, we observe that the amplitude of the inward unitary current diminishes as the membrane is further and further depolarized (see Figure 4.11a). In other words, the net entry of Na<sup>+</sup> ions through a single channel diminishes as the membrane depolarizes. The  $i_{\text{Na}}-V$  relation is obtained by plotting the amplitude of the unitary current ( $i_{\text{Na}}$ ) versus membrane potential ( $V_m$ ). It is linear between  $-50 \text{ mV}$  and  $0 \text{ mV}$  (Figure 4.9a). For membrane potentials more hyperpolarized than  $-50 \text{ mV}$ , there are no values of  $i_{\text{Na}}$  since the channel rarely opens or does not open at all. Quantitative data for potentials more depolarized than  $0 \text{ mV}$  are not available.

The critical point of the current-voltage relation is the membrane potential for which the current is zero; i.e. the reversal potential of the current ( $E_{\text{rev}}$ ). If only Na<sup>+</sup> ions flow through the Na<sup>+</sup> channel, the reversal potential is equal to  $E_{\text{Na}}$ . From  $-50 \text{ mV}$  to  $E_{\text{rev}}$ ,  $i_{\text{Na}}$  is inward and its amplitude decreases. This results from the decrease of the Na<sup>+</sup> driving force ( $V_m - E_{\text{Na}}$ ) as the membrane approaches the reversal potential for Na<sup>+</sup> ions. For membrane potentials more depolarized than  $E_{\text{rev}}$ ,  $i_{\text{Na}}$  is now outward (not shown). Above  $E_{\text{rev}}$ , the amplitude of the outward Na<sup>+</sup> current progressively increases as the driving force for the exit of Na<sup>+</sup> ions increases.

The linear  $i_{\text{Na}}-V$  relation is described by the equation  $i_{\text{Na}} = \gamma_{\text{Na}}(V_m - E_{\text{Na}})$ , where  $V_m$  is the test potential,  $E_{\text{Na}}$  is the reversal potential of the Na<sup>+</sup> current, and  $\gamma_{\text{Na}}$  is the conductance of a single Na<sup>+</sup> channel (unitary conductance). The value of  $\gamma_{\text{Na}}$  is given by the slope of the linear  $i_{\text{Na}}/V$  curve. It has a constant value at any given membrane potential. This value varies between  $5$  and  $18 \text{ pS}$  depending on the preparation.

#### 4.2.5 The probability of the Na<sup>+</sup> channel being in the open state increases with depolarization to a maximal level

An important observation at the single channel level is that the more the membrane is depolarized, the higher is the probability that the Na<sup>+</sup> channel will open. This observation can be made from two types of experiments:

- The activity of a single Na<sup>+</sup> channel is recorded in patch clamp (cell-attached patch). Each depolarizing step is repeated several times and the number of times the Na<sup>+</sup> channel opens is observed (Figure 4.10a). With depolarizing steps to  $-70 \text{ mV}$  from a holding potential of  $-120 \text{ mV}$ , the channel very rarely

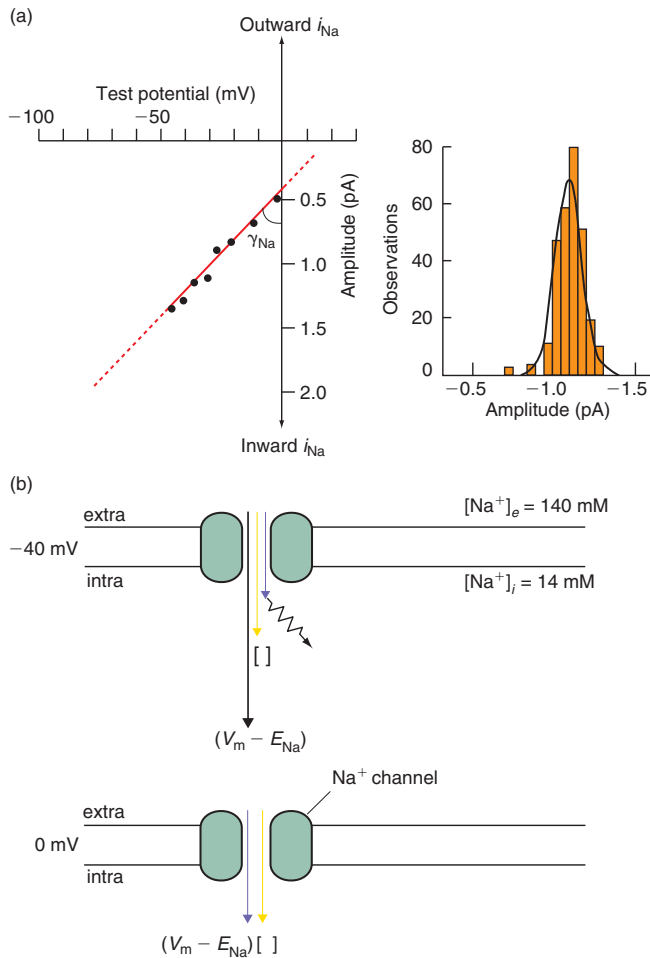


**FIGURE 4.9** The single-channel current/voltage ( $i_{Na}/V$ ) relation is linear.

(a) The activity of the rat type II Na<sup>+</sup> channel expressed in *Xenopus* oocytes from cDNA is recorded in patch clamp (cell-attached patch). Plot of the unitary current amplitude versus test potential: each point represents the mean of 20–200 unitary current amplitudes measured at one potential (left) as shown at  $-32$  mV (right). The relation is linear between test potentials  $-50$  and  $0$  mV (holding potential =  $-90$  mV). The slope is  $\gamma_{Na} = 19$  pS. (b) Drawings of an open voltage-gated Na<sup>+</sup> channel to explain the direction and amplitude of the net flux of Na<sup>+</sup> ions at two test potentials ( $-40$  and  $0$  mV). [ ], force due to the concentration gradient across the membrane;  $\sim\sim\sim\rightarrow$ , force due to the electric gradient;  $V - E_{Na}$ , driving force. The solution bathing the extracellular side of the patch or intrapipette solution contains (in mM): 115 NaCl, 2.5 KCl, 1.8 CaCl<sub>2</sub>, 10 HEPES. Plot (a) adapted from Stühmer W, Methfessel C, Sakmann B *et al.* (1987) Patch clamp characterization of sodium channels expressed from rat brain cDNA. *Eur. Biophys. J.* **14**, 131–138, with permission.

opens; and if it does, the time spent in the open state is very short. In contrast, with depolarizing steps to  $-40$  mV, the Na<sup>+</sup> channels open for each trial.

- The activity of two or three Na<sup>+</sup> channels is recorded in patch clamp (cell-attached patch). In response to depolarizing steps of small amplitude, Na<sup>+</sup> channels do not open or only one Na<sup>+</sup> channel opens at a time. With larger depolarizing steps, the

overlapping currents of two or three Na<sup>+</sup> channels can be observed, meaning that this number of Na<sup>+</sup> channels open with close delays in response to the step (not shown).

From the recordings of **Figure 4.10a**, we can observe that the probability of the Na<sup>+</sup> channel being in the open state varies with the value of the test potential. It also varies with time during the depolarizing step: openings occur more frequently at the beginning of the step. The open probability of Na<sup>+</sup> channels is voltage- and time-dependent. By averaging a large number of records obtained at each test potential, the open probability ( $p_t$ ) of the Na<sup>+</sup> channel recorded can be obtained at each time  $t$  of the step (**Figure 4.10b**). We observe from these curves that after 4–6 ms the probability of the Na<sup>+</sup> channel being in the open state is very low, even with large depolarizing steps: the Na<sup>+</sup> channel inactivates in 4–6 ms. When we compare now the open probabilities at the different test potentials, we observe that the probability of the Na<sup>+</sup> channel being in the open state at time  $t = 2$  ms increases with the amplitude of the depolarizing step.

#### 4.2.6 The macroscopic Na<sup>+</sup> current ( $I_{Na}$ ) has a steep voltage dependence of activation and inactivates within a few milliseconds

The macroscopic Na<sup>+</sup> current,  $I_{Na}$ , is the sum of the unitary currents,  $i_{Na}$ , flowing through all the open Na<sup>+</sup> channels of the recorded membrane

At the axon initial segment or at nodes of Ranvier, there are  $N$  Na<sup>+</sup> channels that can be activated. We have seen that the unitary Na<sup>+</sup> current flowing through a single Na<sup>+</sup> channel has a rectangular shape. What is the time course of the macroscopic Na<sup>+</sup> current,  $I_{Na}$ ?

If we assume that the Na<sup>+</sup> channels in one cell are identical and function independently, the sum of many recordings from the same Na<sup>+</sup> channel should show the same properties as the macroscopic Na<sup>+</sup> current measured from thousands of channels with the voltage clamp technique. In **Figure 4.7b**, an average of 300 unitary Na<sup>+</sup> currents elicited by a 40 mV depolarizing pulse is shown. For a given potential, the ‘averaged’ inward Na<sup>+</sup> current has a fast rising phase and presents a peak at the time  $t = 1.5$  ms. The peak corresponds to the time when most of the Na<sup>+</sup> channels are opened at each trial. Then the averaged current decays with time because the Na<sup>+</sup> channel has a low probability of being in the open state later in the step (owing to the inactivation of the Na<sup>+</sup> channel). At each trial, the Na<sup>+</sup> channel does not inactivate exactly at the same time, which explains the progressive decay of the averaged macroscopic Na<sup>+</sup> current. A similar averaged Na<sup>+</sup> current is shown

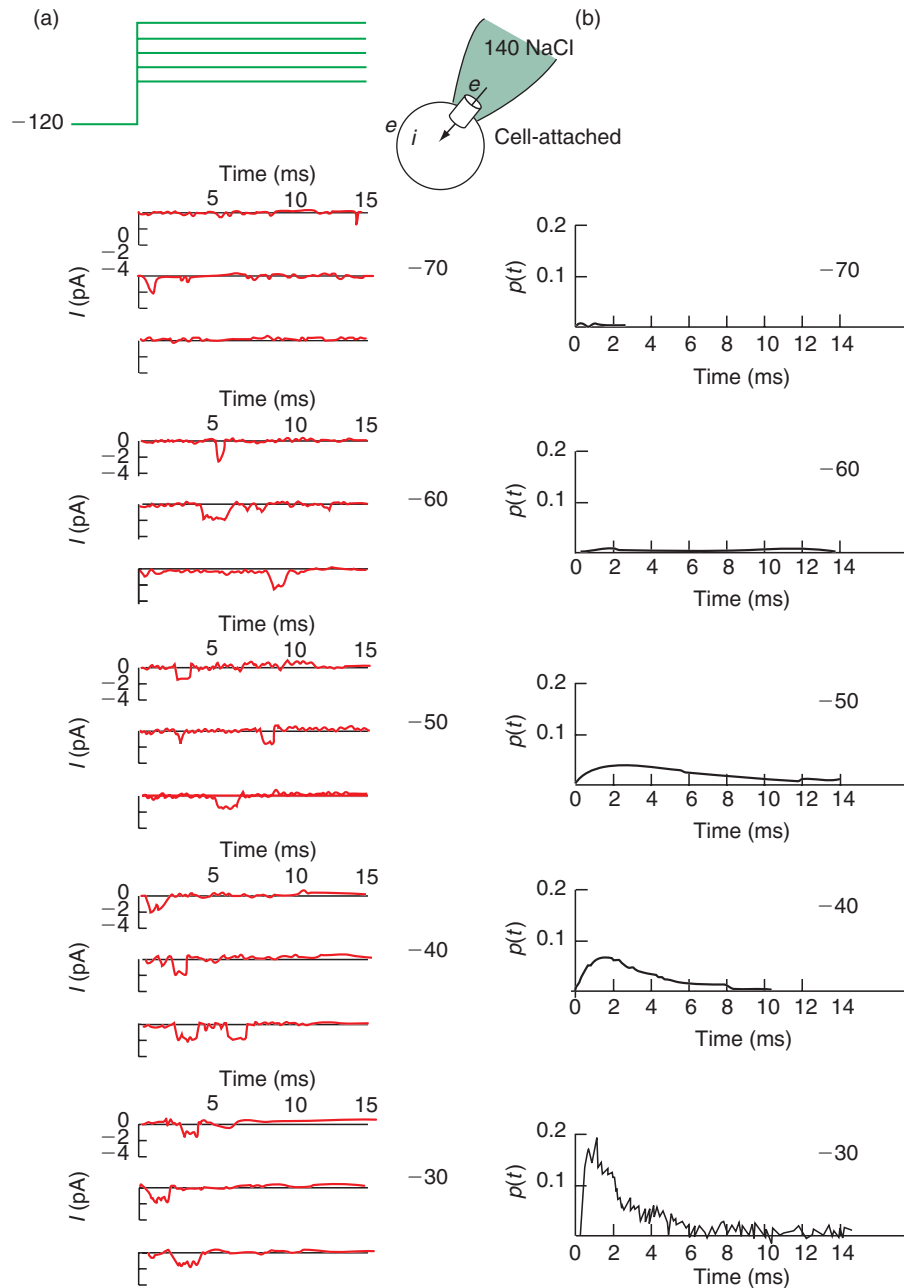


**FIGURE 4.10** The open probability of the voltage-gated  $\text{Na}^+$  channel is voltage- and time-dependent.

Single  $\text{Na}^+$  channel activity recorded in a mammalian neuroblastoma cell in patch clamp (cell-attached patch). **(a)** In response to a depolarizing step to the indicated potentials from a holding potential of  $-120$  mV, unitary inward currents are recorded. **(b)** Ensemble of averages of single-channel openings at the indicated voltages; 64 to 2000 traces are averaged at each voltage to obtain the time-dependent open probability of a channel ( $p(t)$ ) in response to a depolarization. The open probability at time  $t$  is calculated according to the equation:  $p(t) = I_{\text{Na}(t)} / N i_{\text{Na}}$ , where  $I_{\text{Na}(t)}$  is the average current at time  $t$  at a given voltage,  $N$  is the number of channels (i.e. the number of averaged recordings of single channel activity) and  $i_{\text{Na}}$  is the unitary current at a given voltage. At  $-30$  mV the open probability is maximum. The channels inactivate in 4 ms. Adapted from Aldrich RW and Steven CF (1987) Voltage-dependent gating of sodium channels from mammalian neuroblastoma cells. *J. Neurosci.* 7, 418–431, with permission.

in **Figure 4.8b**. The averaged current does not have a rectangular shape because the  $\text{Na}^+$  channel does not open with the same delay and does not inactivate at the same time at each trial.

The *averaged* macroscopic  $\text{Na}^+$  current has a time course similar to that of the *recorded* macroscopic  $\text{Na}^+$  current from the same type of cell at the same potential. However, the averaged current from 300  $\text{Na}^+$  channels

still presents some angles in its time course. In contrast, the macroscopic recorded Na<sup>+</sup> current is smooth. The more numerous are the Na<sup>+</sup> channels opened by the depolarizing step, the smoother is the total Na<sup>+</sup> current. The value of  $I_{\text{Na}}$  at each time  $t$  at a given potential is:

$$I_{\text{Na}} = Np_{(t)}i_{\text{Na}}$$

where  $N$  is the number of Na<sup>+</sup> channels in the recorded membrane and  $p_{(t)}$  is the open probability at time  $t$  of the Na<sup>+</sup> channel; it depends on the membrane potential and on the channel opening and inactivating rate constants.  $i_{\text{Na}}$  is the unitary Na<sup>+</sup> current and  $Np_{(t)}$  is the number of Na<sup>+</sup> channels open at time  $t$ .

The  $I_{\text{Na}}-V$  relation is bell-shaped though the  $i_{\text{Na}}-V$  relation is linear

We have seen that the amplitude of the unitary Na<sup>+</sup> current decreases linearly with depolarization (see **Figure 4.9a**). In contrast, the  $I_{\text{Na}}-V$  relation is not linear. The macroscopic Na<sup>+</sup> current is recorded from a myelinated rabbit nerve with the double electrode voltage clamp technique. When the amplitude of the peak Na<sup>+</sup> current is plotted against membrane potential, it has a clear bell shape (**Figures 4.11** and **4.12a**).

Analysis of each trace from the smallest depolarizing step to the largest shows that:

- For small steps, the peak current amplitude is small (0.2 nA) and has a slow time to peak (1 ms). At these potentials the Na<sup>+</sup> driving force is strong but the Na<sup>+</sup> channels have a low probability of opening (**Figure 4.11a**). Therefore,  $I_{\text{Na}}$  is small since it represents the current through a small number of open Na<sup>+</sup> channels. Moreover, the small number of activated Na<sup>+</sup> channels open with a delay since the depolarization is just *subliminal*. This explains the slow time to peak.
- As the depolarizing steps increase in amplitude (to  $-42/-35$  mV), the amplitude of  $I_{\text{Na}}$  increases to a maximum ( $-3$  nA) and the time to peak decreases to a minimum (0.2 ms). Larger depolarizations increase the probability of the Na<sup>+</sup> channel being in the open state and shorten the delay of opening (see **Figure 4.10**). Therefore, though the amplitude of  $i_{\text{Na}}$  decreases between  $-63$  and  $-35$  mV, the amplitude of  $I_{\text{Na}}$  increases owing to the large increase of open Na<sup>+</sup> channels.
- After this peak, the amplitude of  $I_{\text{Na}}$  decreases to zero since the open probability does not increase enough to compensate for the decrease of  $i_{\text{Na}}$ . The reversal potential of  $I_{\text{Na}}$  is the same as that of  $i_{\text{Na}}$  since it depends only on the extracellular and intracellular concentrations of Na<sup>+</sup> ions.

- $I_{\text{Na}}$  changes polarity for  $V_m$  more depolarized than  $E_{\text{rev}}$ : it is now an outward current whose amplitude increases with the depolarization (**Figure 4.10b**).

It is important to note that membrane potentials more depolarized than  $+20$  mV are non-physiological.

*Activation and inactivation curves: the threshold potential*

Activation rate is the rate at which a macroscopic current turns on in response to a depolarizing voltage step. The Na<sup>+</sup> current is recorded in a voltage clamp from a node of rabbit nerve. Depolarizing steps from  $-70$  mV to  $+20$  mV are applied from a holding potential of  $-80$  mV. When the ratio of the peak current at each test potential to the maximal peak current ( $I_{\text{Na}}/I_{\text{Na,max}}$ ) is plotted against test potential, the activation curve of  $I_{\text{Na}}$  can be visualized. The distribution is fitted by a sigmoidal curve (**Figure 4.12b**). In this preparation, the threshold of Na<sup>+</sup> channel activation is  $-60$  mV. At  $-40$  mV,  $I_{\text{Na}}$  is already maximal ( $I_{\text{Na}}/I_{\text{Na,max}} = 1$ ). This steepness of activation is a characteristic of the voltage-gated Na<sup>+</sup> channels.

Inactivation of a current is the decay of this current during a maintained depolarization. To study inactivation, the membrane is held at varying holding potentials and a depolarizing step to a fixed value is applied where  $I_{\text{Na}}$  is maximal (0 mV for example). The amplitude of the peak Na<sup>+</sup> current is plotted against the holding potential.  $I_{\text{Na}}$  begins to inactivate at  $-90$  mV and is fully inactivated at  $-50$  mV. Knowing that the resting membrane potential in this preparation is around  $-80$  mV, some of the Na<sup>+</sup> channels are already inactivated at rest.

*Ionic selectivity of the Na<sup>+</sup> channel*

To compare the permeability of the Na<sup>+</sup> channel to several monovalent cations, the macroscopic current is recorded at different membrane potentials in the presence of external Na<sup>+</sup> ions and when all the external Na<sup>+</sup> are replaced by a test cation. Lithium is as permeant as sodium but K<sup>+</sup> ions are weakly permeant ( $P_{\text{K}}/P_{\text{Na}} = 0.048$ ). Therefore, Na<sup>+</sup> channels are highly selective for Na<sup>+</sup> ions and only 4% of the current is carried by K<sup>+</sup> ions (**Figure 4.13**).

*Tetrodotoxin is a selective open Na<sup>+</sup> channel blocker*

A large number of biological toxins can modify the properties of the Na<sup>+</sup> channels. One of these, tetrodotoxin (TTX), which is found in the liver and ovaries of the pufferfishes, (tetrodon) totally abolishes the current through most of the Na<sup>+</sup> channels (TTX sensitive Na<sup>+</sup>

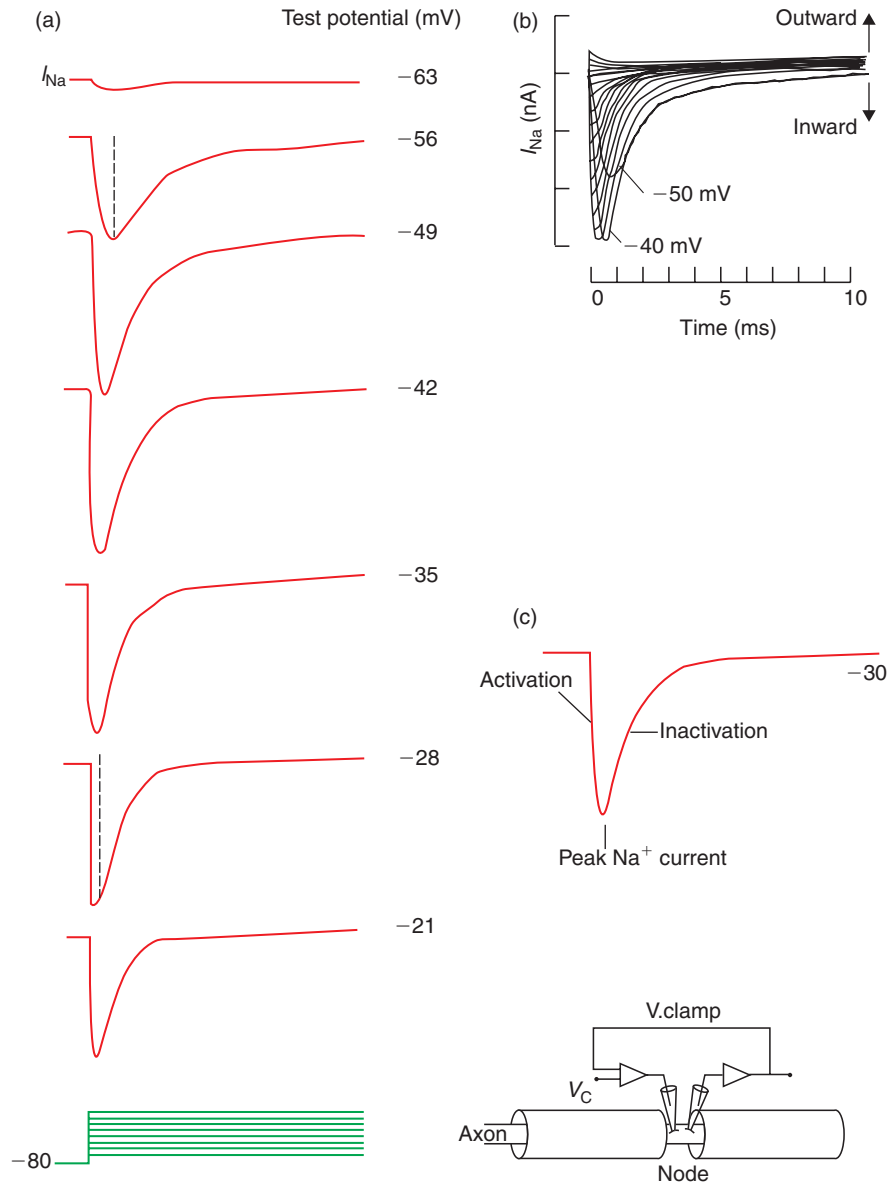


**FIGURE 4.11 Voltage dependence of the macroscopic voltage-gated  $\text{Na}^+$  current.**

The macroscopic voltage-gated  $\text{Na}^+$  current recorded in a node of a rabbit myelinated nerve in voltage clamp conditions. **(a)** Depolarizing steps from  $-70$  mV to  $-21$  mV from a holding potential of  $-80$  mV evoke macroscopic  $\text{Na}^+$  currents ( $I_{\text{Na}}$ ) with different time courses and peak amplitudes. The test potential is on the right. Bottom trace is the voltage trace. **(b)** The traces in (a) are superimposed and current responses to depolarizing steps from  $-14$  to  $+55$  mV are added. The outward current traces are recorded when the test potential is beyond the reversal potential ( $+30$  mV in this preparation). **(c)**  $I_{\text{Na}}$  recorded at  $-30$  mV. The rising phase of  $I_{\text{Na}}$  corresponds to activation of the  $\text{Na}^+$  channels and the decrease of  $I_{\text{Na}}$  corresponds to progressive inactivation of the open  $\text{Na}^+$  channels. The extracellular solution contains (in mM): 154 NaCl, 2.2  $\text{CaCl}_2$ , 5.6 KCl; pH 7.4. Adapted from Chiu SY, Ritchie JM, Bogart RB, Stagg D (1979) A quantitative description of membrane currents from a rabbit myelinated nerve. *J. Physiol.* 292, 149–166, with permission.

channels) (**Figure 4.4**). However, some  $\text{Na}^+$  channels are resistant to TTX such as those from the pufferfishes. TTX has a binding site supposed to be located near the extracellular mouth of the pore.

A single point mutation of the rat brain  $\text{Na}^+$  channel type II, which changes the glutamic acid residue 387 to glutamine (E387Q) in the repeat I, renders the channel insensitive to concentrations of TTX up to tens of

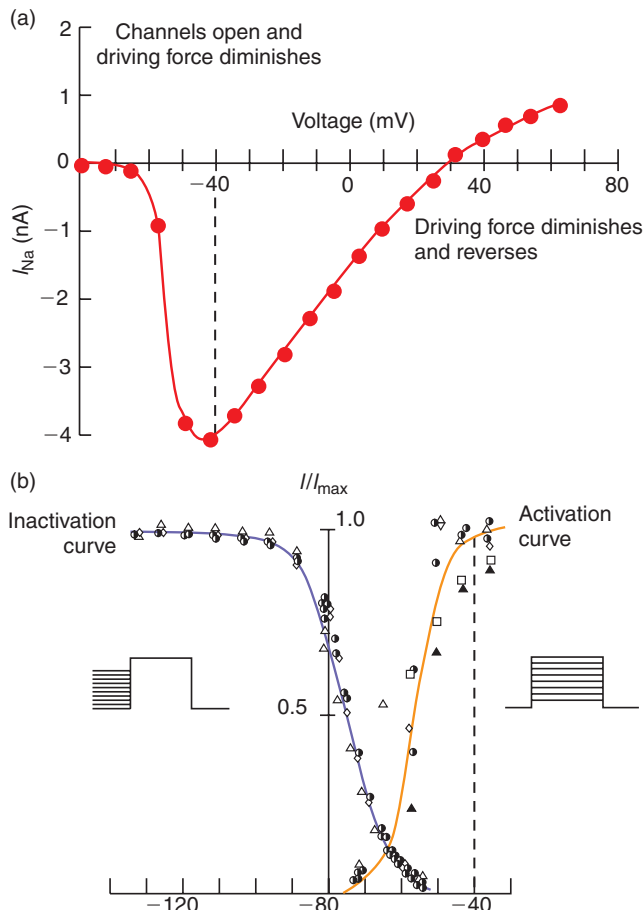


**FIGURE 4.12** Activation-inactivation properties of the macroscopic voltage-gated  $\text{Na}^+$  current.

The  $I_{\text{Na}}-V$  relation has a bell shape with a peak at  $-40$  mV and a reversal potential at  $+30$  mV (the average  $E_{\text{Na}}$  in the rabbit node is  $+27$  mV). (b) Activation (right curve) and inactivation (left curve) curves obtained from nine different experiments. The voltage protocols used are shown in insets. In the ordinates,  $I/I_{\text{max}}$  represents the ratio of the peak  $\text{Na}^+$  current ( $I$ ) recorded at the tested potential of the abscissae and the maximal peak  $\text{Na}^+$  current ( $I_{\text{max}}$ ) recorded in this experiment. It corresponds in the activation curve to the peak current recorded at  $-40$  mV in Figure 4.11. From Chiu SY, Ritchie JM, Bogart RB, Stagg D (1979) A quantitative description of membrane currents from a rabbit myelinated nerve. *J. Physiol.* **292**, 149–166, with permission.

micromolar. *Xenopus* oocytes are injected with the wild-type mRNA or the mutant mRNA and the whole cell  $\text{Na}^+$  currents are recorded with the double-electrode voltage clamp technique. TTX sensitivity is assessed by perfusing TTX-containing external solutions and by measuring the peak of the whole-cell inward  $\text{Na}^+$  current (the peak means the maximal amplitude of the inward  $\text{Na}^+$  current measured on the  $I_{\text{Na}}/V$  relation). The dose-response curves of **Figure 4.14** show that  $1 \mu\text{M}$  of TTX completely abolishes the wild-type  $\text{Na}^+$  current, but has no effect on the mutant  $\text{Na}^+$  current. The other characteristics of the  $\text{Na}^+$  channel are not

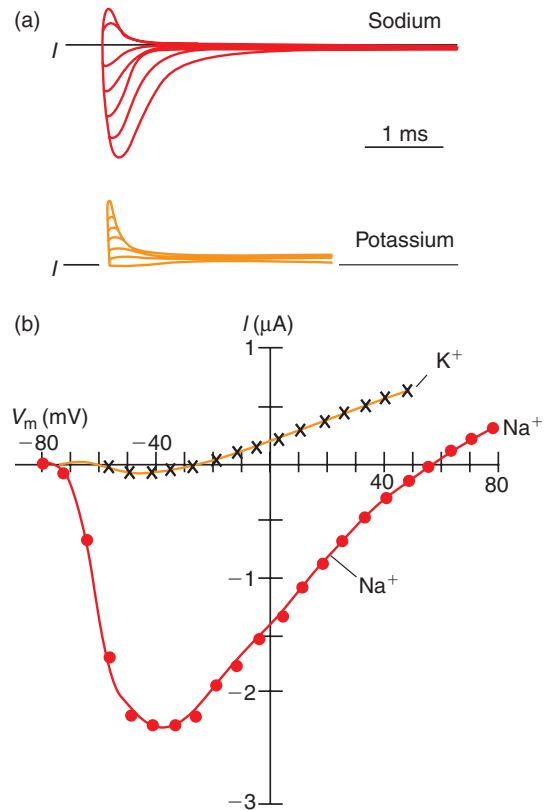


**FIGURE 4.13** Ionic selectivity of the  $\text{Na}^+$  channel.

(a) The macroscopic  $\text{Na}^+$  current is recorded with the double-electrode voltage clamp technique in a mammalian skeletal muscle fibre at different test membrane potentials (from  $-70$  to  $+80$  mV) from a holding potential of  $-80$  mV. (a) Inward currents in normal  $\text{Na}^+$ -Ringer (sodium) and in a solution where all  $\text{Na}^+$  ions are replaced by  $\text{K}^+$  ions (potassium). The other voltage-gated currents are blocked. (b)  $I-V$  relation of the currents recorded in (a).  $I$  is the amplitude of the peak current at each tested potential. Adapted from Pappone PA (1980) Voltage clamp experiments in normal and denervated mammalian skeletal muscle fibers. *J Physiol.* **306**, 377–410, with permission.

significantly affected, except for a reduction in the amplitude of the inward current at all potentials tested. All these results suggest that the link between segments S5 and S6 in repeat I of the rat brain  $\text{Na}^+$  channel is in close proximity to the channel mouth.

Comparison of the predicted protein sequences of the skeletal muscle sodium channels show that pufferfish  $\text{Na}^+$  channels have accumulated several unique substitutions in the otherwise highly conserved pore loop regions of the four domains. Among these substitutions, some are associated with TTX resistance as assessed with patch clamp recordings. What advantages does TTX resistance offer pufferfishes? A main advantage is that the high tissue concentrations of TTX act as an effective chemical defense against predators. Also TTX resistance

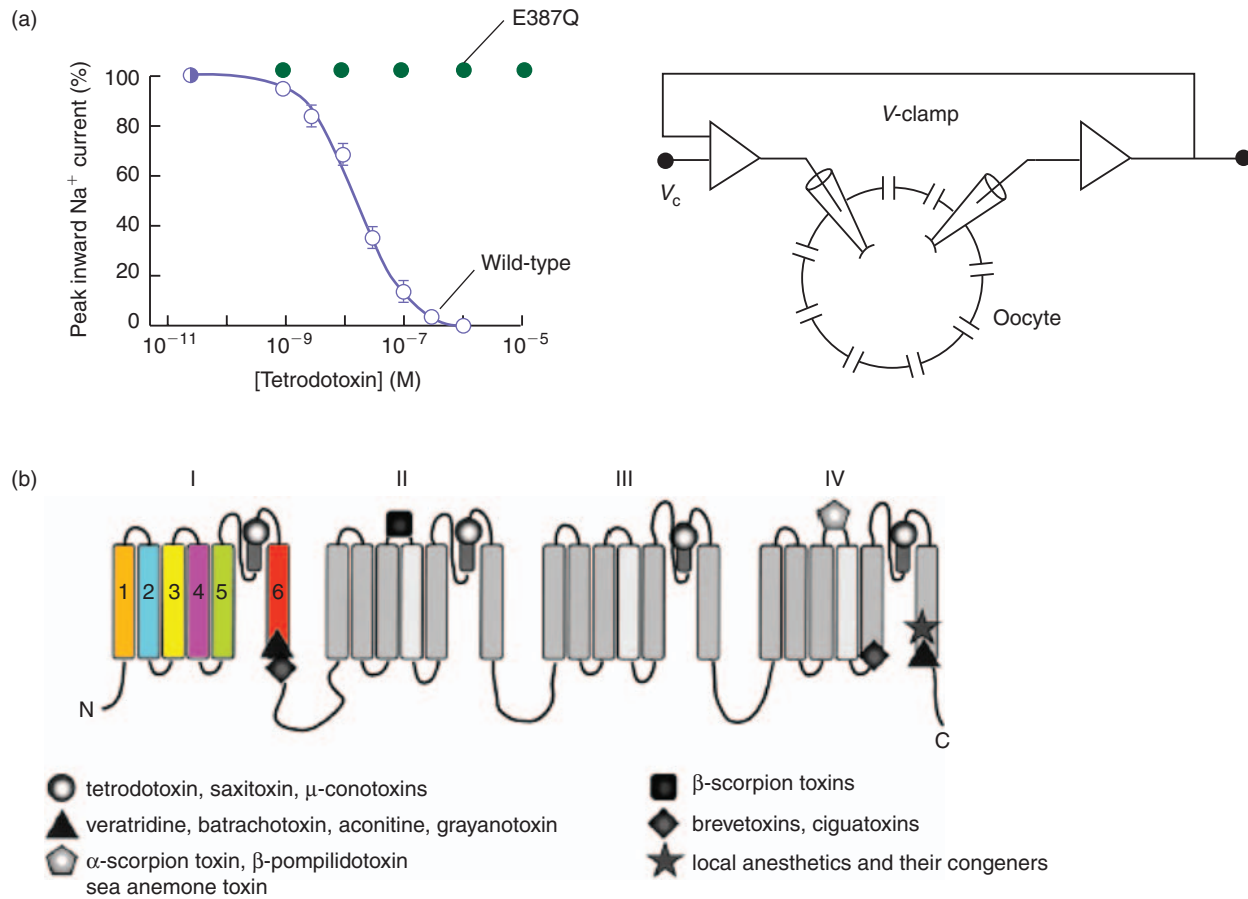


**FIGURE 4.14** A single mutation close to the S6 segment of repeat I completely suppresses the sensitivity of the  $\text{Na}^+$  channel to TTX.

(a) A mutation of the glutamic acid residue 387 to glutamine (E387Q) is introduced in the rat  $\text{Na}^+$  channel type II. *Xenopus* oocytes are injected with either the wild-type mRNA or the mutant mRNA. The macroscopic  $\text{Na}^+$  currents are recorded 4–7 days later with the double-electrode voltage clamp technique. Dose-response curves for the wild-type (open circles) and the mutant E387Q (filled circles) to tetrodotoxin (TTX). TTX sensitivity is determined by perfusing TTX-containing external solutions and by measuring the macroscopic peak inward current. The TTX concentration that reduces the wild-type  $\text{Na}^+$  current by 50% ( $\text{IC}_{50}$ ) is 18 nM. Data are averaged from 7–8 experiments. (b) Topology of drug binding sites on  $\text{Na}^+$  channel  $\alpha$ -subunit. Each symbol represents the toxin or drug binding site indicated at the bottom of the figure. All these sites have been characterized by site-directed mutagenesis. Part (a) from Noda M, Suzuki H, Numa S, Stühmer W (1989) A single point mutation confers tetrodotoxin and saxitoxin insensitivity on the sodium channel II. *FEBS Lett.* **259**, 213–216, with permission. Part (b) drawing adapted from Ogata N and Ohishi Y (2002) Molecular diversity of structure and function of the voltage-gated  $\text{Na}^+$  channels. *Jpn. J. Pharmacol.* **88**, 365–377.

enables pufferfishes to feed on TTX-bearing organisms that are avoided by other fishes.

TTX is not the only toxin to target  $\text{Na}^+$  channels. Most of these toxins, except for TTX and its congeners that occlude the outer pore of the channel, bind to sites that are related to activation and inactivation processes. They fall into at least five different classes according to their corresponding receptor sites:

(1) hydrophilic toxins such as TTX, saxitoxin (STX) and  $\alpha$ -conus toxin; (2) lipid-soluble neurotoxins such as batrachotoxin (BTX), veratridine, aconitine and grayanotoxin; (3)  $\alpha$ -scorpion peptide toxins and sea anemone peptide toxins; (4)  $\beta$ -scorpion peptide toxins; (5) lipid-soluble brevetoxins and ciguatoxins. They can have opposite effects. For example, toxins (2) are activators of  $\text{Na}^+$  channels.

#### 4.2.7 Segment S4, the region between segments S5 and S6, and the region between domains III and IV play a significant role in activation, ion permeation and inactivation, respectively

The major questions about a voltage-gated ionic channel and particularly the Na<sup>+</sup> channel are the following:

- How does the channel open in response to a voltage change?
- How is the permeation pathway designed to define single-channel conductance and ion selectivity?
- How does the channel inactivate?

In order to identify regions of the Na<sup>+</sup> channels involved in these functions, site-directed mutagenesis experiments were performed. The activity of each type of mutated Na<sup>+</sup> channel is analyzed with patch clamp recording techniques.

*The short segments between putative membrane spanning segments S5 and S6 are membrane associated and contribute to pore formation*

The Na<sup>+</sup> channels are highly selective for Na<sup>+</sup> ions. This selectivity presumably results from negatively charged amino acid residues located in the channel pore. Moreover, these amino acids must be specific to Na<sup>+</sup> channels (i.e. different from the other members of voltage-gated cationic channels such as K<sup>+</sup> and Ca<sup>2+</sup> channels) to explain their weak permeability to K<sup>+</sup> or Ca<sup>2+</sup> ions.

Studies using mutagenesis to alter ion channel function have shown that the region connecting the S5 and S6 segments forms part of the channel lining (see **Figure 4.6**). A single amino acid substitution in these regions in repeats III and IV alters the ion selectivity of the Na<sup>+</sup> channel to resemble that of Ca<sup>2+</sup> channels. These residues would constitute part of the selectivity filter of the channel. There is now a general agreement that the selectivity filter is formed by pore loops; i.e. relatively short polypeptide segments that extend into the aqueous pore from the extracellular side of the membrane. Rather than extending completely across the lipid bilayer, a large portion of the pore loop is near the extracellular face of the channel. Only a short region extends into the membrane to form the selectivity filter. In the case of the voltage-gated Na<sup>+</sup> channel, each of the four homologous domains contributes a loop to the ion conducting pore.

*The S4 segment is the voltage sensor*

The S4 segments are positively charged and hydrophobic (**Figure 4.15a**). Moreover, the typical amino

acid sequence of S4 is conserved among the different voltage-gated channels. These observations led to the suggestion that S4 segments have a transmembrane orientation and are voltage sensors. To test this proposed role, positively charged amino acid residues are replaced by neutral or negatively charged residues in the S4 segment of a rat brain Na<sup>+</sup> channel type II. The mutated channels are expressed in *Xenopus* oocytes. When more than three positive residues are mutated in the S4 segments of repeat I or II, no appreciable expression of the mutated channel is obtained. The replacement of only one arginine or lysine residue in segment S4 of repeat I by a glutamine residue shifts the activation curve to more positive potentials (**Figure 4.15b, c**).

It is hypothesized that the positive charges in S4 form ion pairs with negative charges in other transmembrane regions, thereby stabilizing the channel in the non-conducting closed conformation. With a change in the electric field across the membrane, these ion pairs would break as the S4 charges move and new ion pairs would form to stabilize the conducting, open conformation of the channel.

*The cytoplasmic loop between domains III and IV contains the inactivation particle which, in a voltage-dependent manner, enters the mouth of the Na<sup>+</sup> channel pore and inactivates the channel*

The results obtained from three different types of experiments strongly suggest that the short cytoplasmic loop connecting homologous domains III and IV, L<sub>III-IV</sub> loop (see **Figures 4.6a** and **4.16a**), is involved in inactivation: (i) cytoplasmic application of endopeptidases; (ii) cytoplasmic injection of antibodies directed against a peptide sequence in the region between repeats III and IV; and (iii) cleavage of the region between repeats III and IV (**Figure 4.16a-c**); all strongly reduce or block inactivation. Moreover, in some human pathology where the Na<sup>+</sup> channels poorly inactivate (as shown with single-channel recordings from biopsies), this region is mutated.

Positively charged amino acid residues of this L<sub>III-IV</sub> loop are not required for inactivation since only the mutation of a hydrophobic sequence, isoleucine-phenylalanine-methionine (IFM), to glutamine completely blocks inactivation. The critical residue of the IFM motif is phenylalanine since its mutation to glutamine slows inactivation 5000-fold. It is proposed that this IFM sequence is directly involved in the conformational change leading to inactivation. It would enter the mouth of the pore, thus occluding it during the process of inactivation. In order to test this hypothesis, the ability of synthetic peptides containing the IFM motif to restore fast inactivation to non-inactivating rat brain Na<sup>+</sup> channels expressed in kidney carcinoma

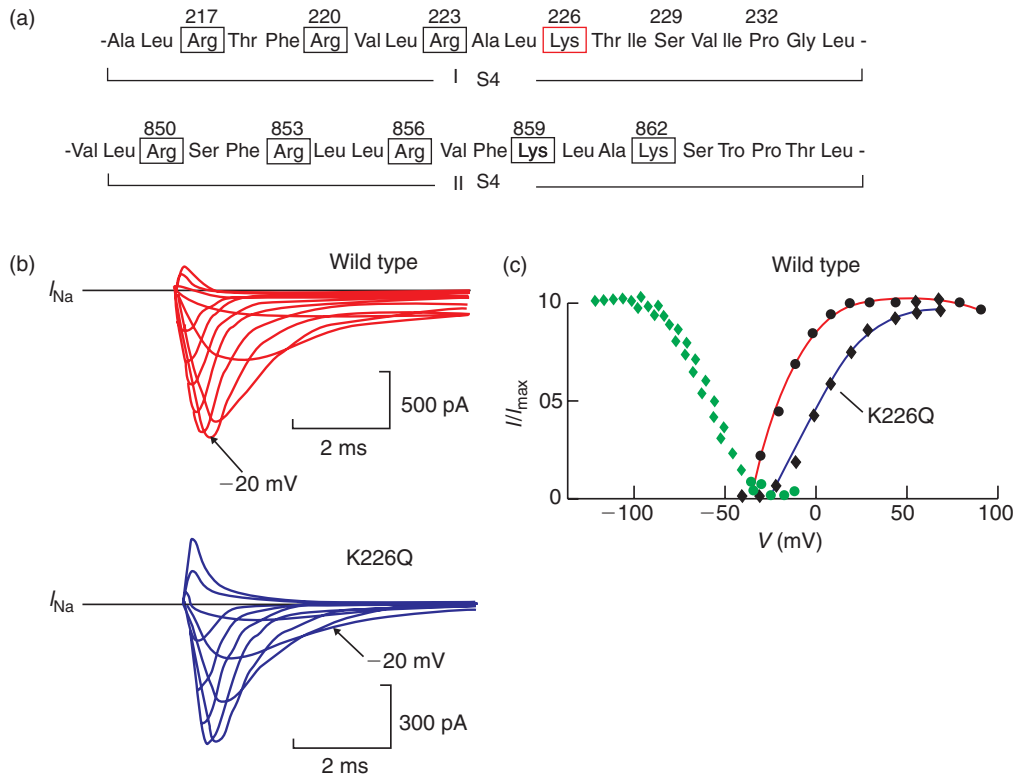


**FIGURE 4.15** Effect of mutations in the S4 segment on Na<sup>+</sup> current activation.

Oocytes are injected with the wild-type rat brain Na<sup>+</sup> channel or with Na<sup>+</sup> channels mutated on the S4 segment. The activity of a population of Na<sup>+</sup> channels is recorded in patch clamp (cell-attached macropatches). (a) Amino acid sequences of segment S4 of the internal repeats I (I S4) and II (II S4) of the wild-type rat Na<sup>+</sup> channel. Positively charged amino acids are boxed with solid lines and the numbers of the relevant residues are given. In the mutated channel studied here the lysine residue in position 226 is replaced by a glutamine residue (K226Q). (b) In response to step depolarizations ranging from -60 to +70 mV from a holding potential of -120 mV, a family of macroscopic Na<sup>+</sup> currents is recorded for each type of Na<sup>+</sup> channel. The arrow indicates the response to the test potential -20 mV. Note that at -20 mV the amplitude of the Na<sup>+</sup> current is at its maximum for the wild-type and less than half maximum for the mutated channel. (c) Steady-state activation (right) and inactivation (left) curves for the wild-type (circles) and the mutant (diamonds) Na<sup>+</sup> channels. Adapted from Stühmer W, Conti F, Suzuki H *et al.* (1989) Structural parts involved in activation and inactivation of the sodium channel. *Nature* 339, 597–603, with permission.

cells is examined. The intrinsic inactivation of Na<sup>+</sup> channels is first made non-functional by a mutation of the IFM motif. When the recording is now performed with a patch pipette containing the synthetic peptide with an IFM motif, the non-inactivating whole cell Na<sup>+</sup> current now inactivates. Since the restored inactivation has the rapid, voltage-dependent time course characteristic of inactivation of the wild-type Na<sup>+</sup> channels, it is proposed that the IFM motif serves as an inactivation particle (Figure 4.16d).

#### 4.2.8 Conclusion: the consequence of the opening of a population of $N$ Na<sup>+</sup> channels is a transient entry of Na<sup>+</sup> ions which depolarizes the membrane above 0 mV

The function of the population of  $N$  Na<sup>+</sup> channels at the axon initial segment or at nodes of Ranvier is to

ensure a *sudden* and *brief* depolarization of the membrane above 0 mV.

#### *Rapid activation of Na<sup>+</sup> channels makes the depolarization phase sudden*

In response to a depolarization to the threshold potential, the closed Na<sup>+</sup> channels (Figure 4.17a) of the axon initial segment begin to open (b). The flux of Na<sup>+</sup> ions through the few open Na<sup>+</sup> channels depolarizes the membrane more and thus triggers the opening of other Na<sup>+</sup> channels (c). In consequence, the flux of Na<sup>+</sup> ions increases, depolarizes the membrane more and opens other Na<sup>+</sup> channels until all the  $N$  Na<sup>+</sup> channels of the segment of membrane are opened (d). In (d) the depolarization phase is at its peak. Na<sup>+</sup> channels are opened by depolarization and once opened, they contribute to the membrane depolarization and therefore to their activation: it is a self-maintained process.

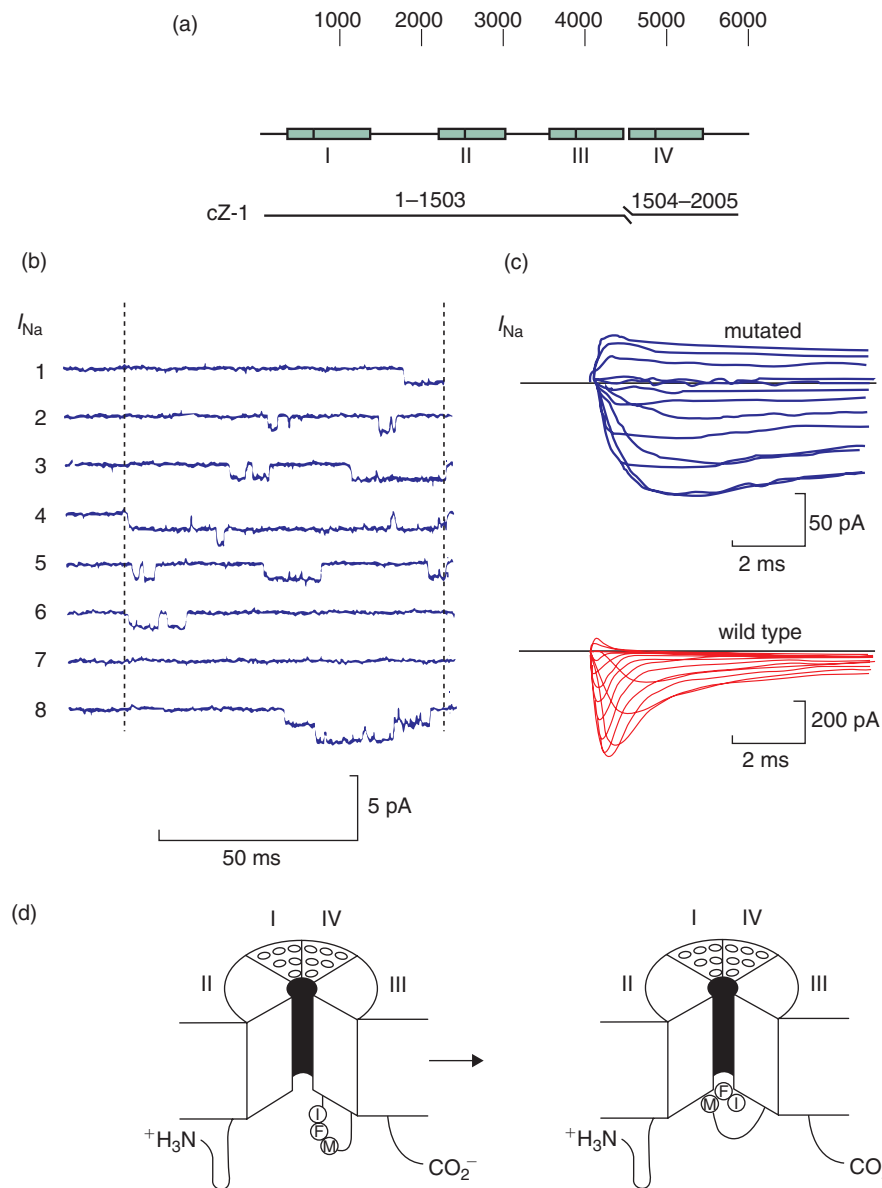


**FIGURE 4.16** Effects of mutations in the region between repeats III and IV on  $\text{Na}^+$  current inactivation. (a) Linear representation of the wild-type  $\text{Na}^+$  channel (upper trace) and the mutated  $\text{Na}^+$  channel (bottom trace). The mutation consists of a cut with an addition of four to eight residues at each end of the cut. An equimolar mixture of the two mRNAs encoding the adjacent fragments of the  $\text{Na}^+$  channel protein separated with a cut is injected in oocytes. (b) Single-channel recordings of the activity of the mutated  $\text{Na}^+$  channel in response to a depolarizing step to  $-20\text{ mV}$  from a holding potential of  $-100\text{ mV}$ . Note that late single or double openings (line 8) are often recorded. The mean open time  $\tau_o$  is  $5.8\text{ ms}$  and the elementary conductance  $\gamma_{\text{Na}}$  is  $17.3\text{ pS}$ . (c) Macroscopic  $\text{Na}^+$  currents recorded from the mutated (upper trace) and the wild-type (bottom trace)  $\text{Na}^+$  channels. (d) Model for inactivation of the voltage-gated  $\text{Na}^+$  channels. The region linking repeats III and IV is depicted as a hinged lid that occludes the transmembrane pore of the  $\text{Na}^+$  channel during inactivation. Parts (a)–(c) from Pappone PA (1980) Voltage clamp experiments in normal and denervated mammalian skeletal muscle fibers. *J Physiol.* **306**, 377–410, with permission. Drawing (d) from West JW, Patton DE, Scheuer T *et al.* (1992) A cluster of hydrophobic amino acid residues required for fast sodium channel inactivation. *Proc. Natl Acad. Sci. USA* **89**, 10910–10914, with permission.

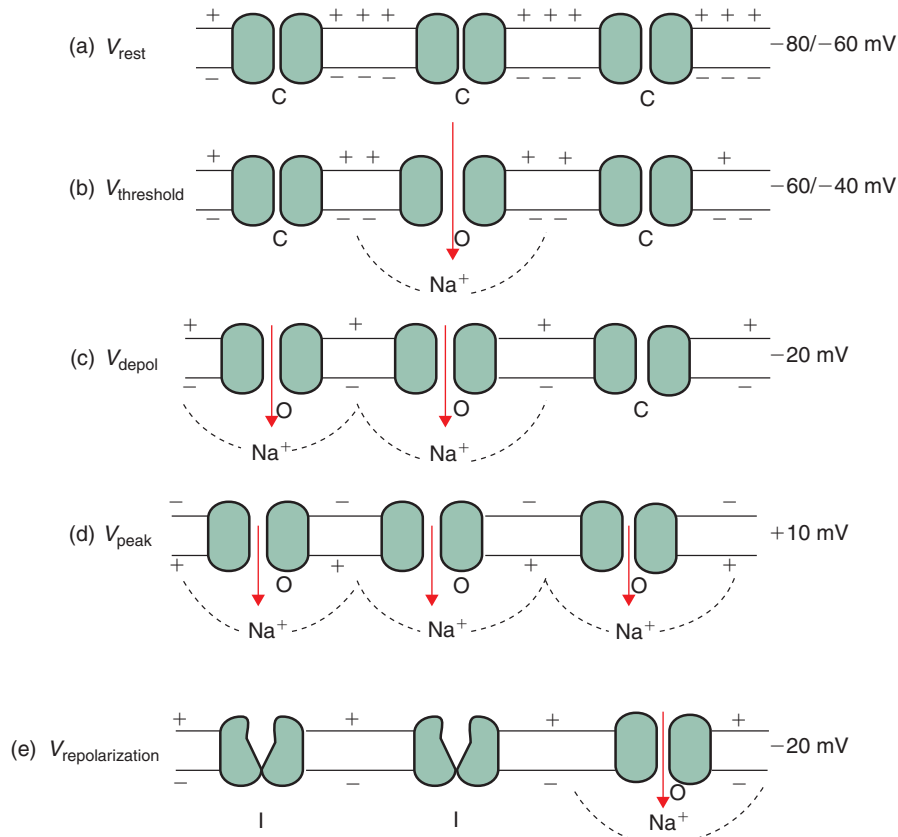


FIGURE 4.17 Different states of voltage-gated  $\text{Na}^+$  channels in relation to the different phases of the  $\text{Na}^+$ -dependent action potential.

C, closed state; O, open state; I, inactivated state;  $\rightarrow$ , driving force for  $\text{Na}^+$  ions.

### *Rapid inactivation of $\text{Na}^+$ channels makes the depolarization phase brief*

Once the  $\text{Na}^+$  channels have opened, they begin to inactivate (e). Therefore, though the membrane is depolarized, the influx of  $\text{Na}^+$  ions diminishes quickly. Therefore the  $\text{Na}^+$ -dependent action potential is a spike and does not present a plateau phase. Inactivation is a very important protective mechanism since it prevents potentially toxic persistent depolarization.

### 4.3 THE REPOLARIZATION PHASE OF THE SODIUM-DEPENDENT ACTION POTENTIAL RESULTS FROM $\text{Na}^+$ CHANNEL INACTIVATION AND PARTLY FROM $\text{K}^+$ CHANNEL ACTIVATION

The participation of a voltage-gated  $\text{K}^+$  current in action potential repolarization differs from one preparation to another. For example, in the squid axon the voltage-gated  $\text{K}^+$  current plays an important role in

spike repolarization, though in mammalian peripheral nerves this current is almost absent. However, the action potentials of the squid axon and that of mammalian nerves have the same duration. This is because the  $\text{Na}^+$  current in mammalian axons inactivates two to three times faster than that of the frog axon. Moreover, the leak  $\text{K}^+$  currents are important in mammalian axons (see below).

Voltage-gated  $\text{K}^+$  channels can be classified into two major groups based on physiological properties:

- Delayed rectifiers which activate after a delay following membrane depolarization and inactivate slowly
- A-type channels which are fast activating and fast inactivating.

The first type, the delayed rectifier  $\text{K}^+$  channels, plays a role in action potential repolarization. The A-types inactivate too quickly to do so. They play a role in firing patterns and are explained in Chapter 14.

This section will explain the structure and activity of the voltage-gated, delayed rectifier  $\text{K}^+$  channels responsible for action potential repolarization in the squid or frog nerves. Then Section 4.4 will explain the other mode

of repolarization observed in mammalian nerves, in which the delayed rectifier current does not play a significant role.

#### 4.3.1 The delayed rectifier K<sup>+</sup> channel consists of four $\alpha$ -subunits and auxiliary $\beta$ -subunits

K<sup>+</sup> channels represent an extremely diverse ion channel type. All known K<sup>+</sup> channels are related members of a single protein family. Finding genes responsible for a native K<sup>+</sup> current is not an easy task, because K<sup>+</sup> channels have a great diversity: more than 100 of K<sup>+</sup> channel subunits have been identified to date. Among strategies used to identify which genes encode a particular K<sup>+</sup> channel are the single cell reverse transcriptase chain reaction (scRT-PCR) protocol combined with patch clamp recording and the injection of subfamily-specific dominant negative constructs in recorded neurons. Results of such experiments strongly suggested that  $\alpha$ -subunits of delayed rectifiers are attributable to Kv2 and Kv3 subfamily genes.

Delayed rectifier K<sup>+</sup> channels  $\alpha$ -subunits form homo- or hetero-tetramers in the cell membrane. As for the Na<sup>+</sup> channel, the P loop linking segments S5 and S6 contributes to the formation of the pore and the auxiliary small  $\beta$ -subunits associated with the  $\alpha$ -subunit are considered to be intracellularly located (Figure 4.18).

#### 4.3.2 Membrane depolarization favours the conformational change of the delayed rectifier channel towards the open state

*The function of the delayed rectifier channel is to transduce, with a delay, membrane depolarization into an exit of K<sup>+</sup> ions*

Single-channel recordings were obtained by Conti and Neher in 1980 from the squid axon. We shall, however, look at recordings obtained from K<sup>+</sup> channels expressed in oocytes or in mammalian cell lines from cDNA encoding a delayed rectifier channel of rat brain. Since the macroscopic currents mediated by these channels have time courses and ionic selectivity resembling those of the classical delayed outward currents described in nerve and muscle, these single-channel recordings are good examples for describing the properties of a delayed rectifier current.

Figure 4.19 shows a current trace obtained from patch clamp recordings (inside-out patch) of a rat brain K<sup>+</sup> channel (RCK1) expressed in a *Xenopus* oocyte. In the presence of physiological extracellular and intracellular K<sup>+</sup> concentrations, a depolarizing voltage step to 0 mV from a holding potential of -60 mV is applied. After the onset of the step, a rectangular pulse of elementary

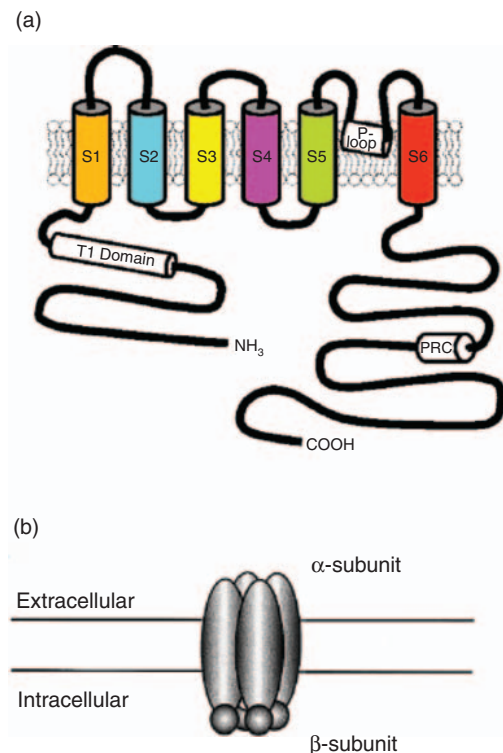


**FIGURE 4.18** Putative transmembrane organization of the  $\alpha$ -subunit of the delayed rectifier, voltage-gated K<sup>+</sup> channel and its associated cytoplasmic  $\beta$ -subunit.

(a) Diagrammatic representation of the predicted membrane topology of a single Kv2.1  $\alpha$ -subunit. S1–S6 represent the transmembrane segments (cylinders represent putative  $\alpha$ -helical segments), P-loop represents the amino acid residues that form the bulk of the lining of the channel pore, T1 domain represents the subfamily-specific tetramerization domain in the cytoplasmic N-terminus, and PRC represents the proximal restriction and clustering signal in the cytoplasmic C-terminus. (b) A schematic diagram showing the putative structure of a voltage-dependent K<sup>+</sup> channel. A channel is composed of four pore-forming  $\alpha$ -subunits, to each of which a  $\beta$ -subunit is associated on the cytoplasmic side. The four  $\alpha$ -subunits can be homomers or heteromers. Part (a) from Misonou H, Mohapatra DP, Trimmer JS (2005) *NeuroToxicology* 26, 743–752, with permission; Part (b) from Song WJ (2002) Genes responsible for native depolarization-activated K<sup>+</sup> currents in neurons. *Neuroscience Research* 42, 7–14.

current, upwardly directed, appears. It means that the current is outward; K<sup>+</sup> ions leave the cell. In fact, the driving force for K<sup>+</sup> ions is outward at 0 mV.

It is immediately striking that the gating behaviour of the delayed rectifier channel is different from that of the Na<sup>+</sup> channel (compare Figures 4.7a or 4.8a and 4.19). Here, the rectangular pulse of current lasts the whole depolarizing step with short interruptions during which the current goes back to zero. It indicates that the delayed rectifier channel opens, closes briefly and reopens many times during the depolarizing pulse: the delayed rectifier channel does not inactivate within seconds. Another difference is that the delay of opening

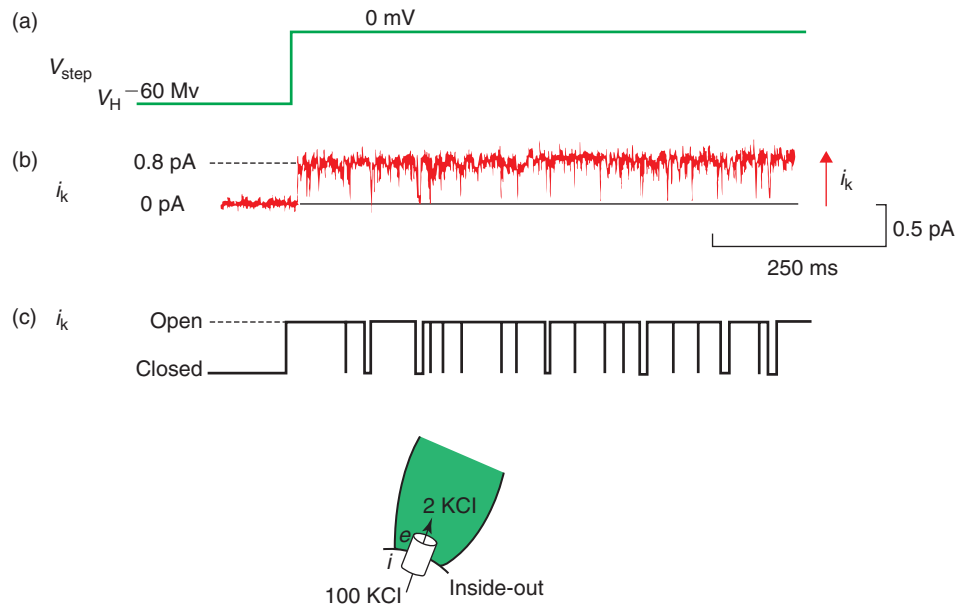


**FIGURE 4.19** Single  $\text{K}^+$  channel openings in response to a depolarizing step.

The activity of a single delayed rectifier channel expressed from rat brain cDNA in a *Xenopus* oocyte is recorded in patch clamp (inside-out patch). A depolarizing step to 0 mV from a holding potential of  $-60$  mV (a) evokes the opening of the channel (b). The elementary current is outward. The channel then closes briefly and reopens several times during the depolarization, as shown in the drawing (c) that interprets the current trace. Bathing solution or intracellular solution (in mM): 100 KCl, 10 EGTA, 10 HEPES. Pipette solution or extracellular solution (in mM): 115 NaCl, 2 KCl, 1.8  $\text{CaCl}_2$ , 10 HEPES. Adapted from Stühmer W, Stocker M, Sakmann B *et al.* (1988) Potassium channels expressed from rat brain cDNA have delayed rectifier properties. *FEBS Lett.* **242**, 199–206, with permission.

of the delayed rectifier is much longer than that of the  $\text{Na}^+$  channel, even for large membrane depolarizations (mean delay 4 ms in **Figure 4.20a**).

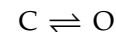
When the same depolarizing pulse is now applied every 1–2 s, we observe that the delay of channel opening is variable (1–10 ms) but gating properties are the same in all recordings: the channel opens, closes briefly and reopens during the entire depolarizing step (**Figure 4.20a**). Amplitude histograms collected at 0 mV membrane potential from current recordings, such as those shown in **Figure 4.20a**, give a mean amplitude of the unitary currents of  $+0.8$  pA (**Figure 4.20c**). This means that the most frequently occurring main amplitude is  $+0.8$  pA.

### 4.3.3 The open probability of the delayed rectifier channel is stable during a depolarization in the range of seconds

The average open time  $\tau_o$  measured in the patch illustrated in **Figure 4.19** is 4.6 ms. The mean closed time  $\tau_c$  is 1.5 ms. As seen in **Figures 4.19** and **4.20a**, during a depolarizing pulse to 0 mV the delayed rectifier channel

spends much more time in the open state than in the closed state: at 0 mV its average open probability is high ( $p_o = 0.76$ ).

In order to test whether the delayed rectifier channels show some inactivation, long-lasting recordings are performed. Though no significant inactivation is apparent during test pulses in the range of seconds, during long test depolarizations (in the range of minutes) the channel shows steady-state inactivation at positive holding potentials (not shown). Therefore, in the range of seconds, the inactivation of the delayed rectifier channel can be omitted: the channel fluctuates between the closed and open states:



The transition from the closed (C) state to the open (O) state is triggered by membrane depolarization with a delay. The delayed rectifier channel activates in the range of milliseconds. In comparison, the  $\text{Na}^+$  channel activates in the range of submilliseconds. The O to C transitions of the  $\text{Na}^+$  channel frequently happen though the membrane is still depolarized. It also happens when membrane repolarizes.

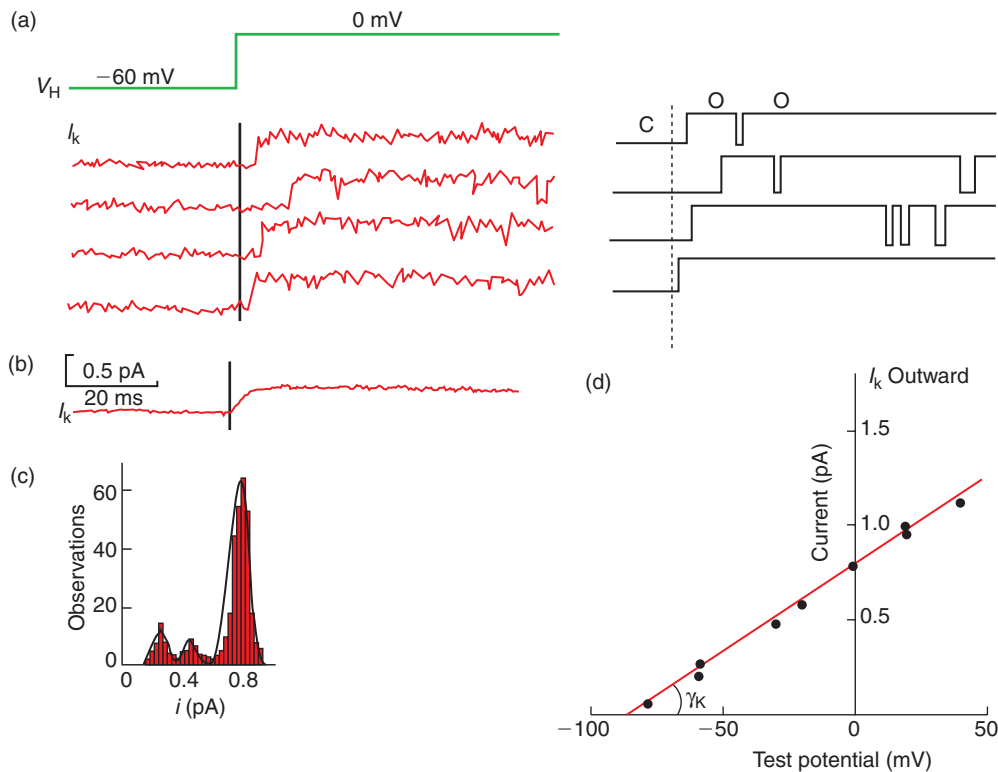


**FIGURE 4.20** Characteristics of the elementary delayed rectifier current.

Same experimental design as in Figure 4.19. The patch of membrane contains a single delayed rectifier channel. (a) Successive sweeps of outward current responses to depolarizing steps from  $-60$  mV to  $0$  mV (C for closed state, O for open state of the channel). (b) Averaged current from 70 elementary currents as in (a). (c) Amplitude histogram of the elementary outward currents recorded at test potential  $0$  mV. The mean elementary current amplitude observed most frequently is  $0.8$  pA. (d) Single channel current–voltage relation ( $i_K - V$ ). Each point represents the mean amplitude of at least 20 determinations. The slope is  $\gamma_K = 9.3$  pS. The reversal potential  $E_{\text{rev}} = -89$  mV. From Stühmer W, Stocker M, Sakmann B *et al.* (1988) Potassium channels expressed from rat brain cDNA have delayed rectifier properties. *FEBS Lett.* **242**, 199–206, with permission.

#### 4.3.4 The $\text{K}^+$ channel has a constant unitary conductance $\gamma_K$

In Figure 4.21a, unitary currents are shown in response to increasing depolarizing steps from  $-50$  to  $+20$  mV from a holding potential of  $-80$  mV. We observe that both the amplitude of the unitary current and the time spent by the channel in the open state increase with depolarization.

When the mean amplitude of the unitary  $\text{K}^+$  current is plotted versus membrane test potential, a linear  $i_K/V$  relation is obtained (Figures 4.20d and 4.21b). This linear  $i_K/V$  relation (between  $-50$  and  $+20$  mV) is described by the equation  $i_K = \gamma_K(V - E_K)$ , where  $V$  is the membrane potential,  $E_K$  is the reversal potential of the  $\text{K}^+$  current, and  $\gamma_K$  is the conductance of the single delayed rectifier  $\text{K}^+$  channel, or unitary conductance. Linear back-extrapolation gives a reversal potential value around  $-90$  /  $-80$  mV, a value close to  $E_K$  calculated from the Nernst equation. This means that from  $-80$  mV

to more depolarized potentials, which correspond to the physiological conditions, the  $\text{K}^+$  current is outward. For more hyperpolarized potentials, the  $\text{K}^+$  current is inward.

The value of  $\gamma_K$  is given by the slope of the linear  $i_K/V$  curve. It has a constant value at any given membrane potential. This value varies between 10 and 15 pS depending on the preparation (Figures 4.20d and 4.21b).

#### 4.3.5 The macroscopic delayed rectifier $\text{K}^+$ current ( $I_K$ ) has a delayed voltage dependence of activation and inactivates within tens of seconds

Whole cell currents in *Xenopus* oocytes expressing delayed rectifier channels start to activate at potentials positive to  $-30$  mV and their amplitude is clearly voltage-dependent. When unitary currents recorded from 70 successive depolarizing steps to  $0$  mV are averaged

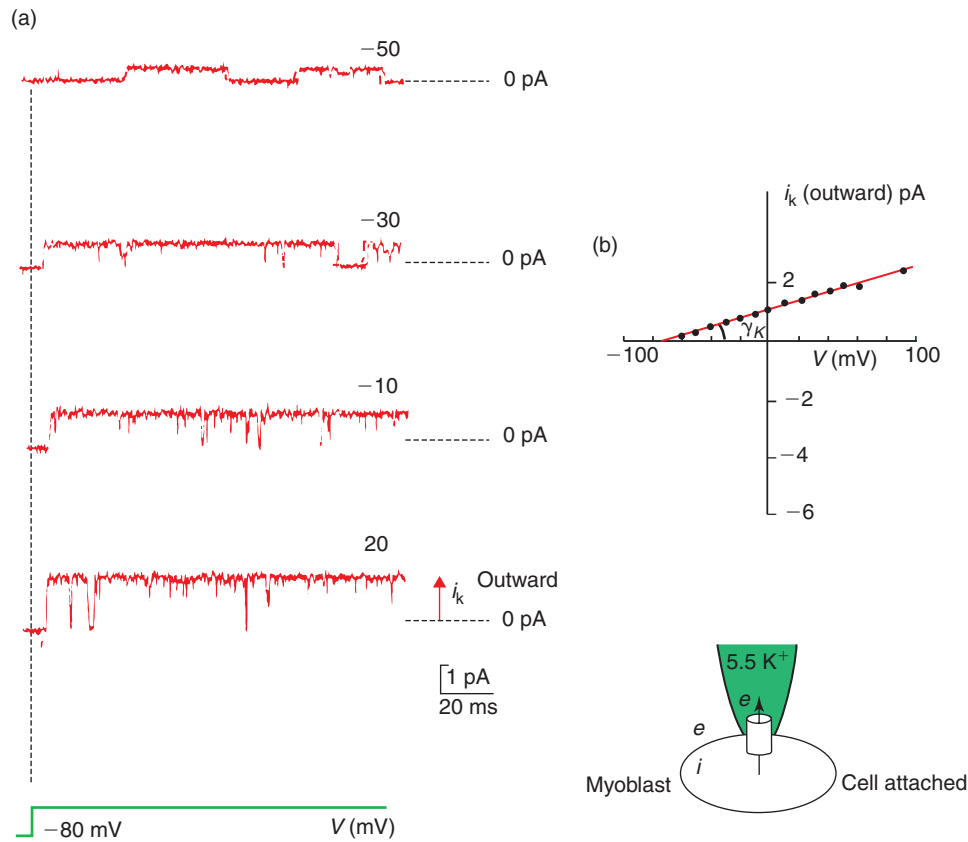


**FIGURE 4.21** The single-channel current/voltage ( $i_K/V$ ) relation is linear.

Delayed rectifier K<sup>+</sup> channels from rat brain are expressed in a myoblast cell line. **(a)** The activity of a single channel is recorded in patch clamp (cell-attached patch). Unitary currents are recorded at different test potentials (from -50 mV to +20 mV) from a holding potential at -80 mV. Bottom trace is the voltage trace. **(b)**  $i_K-V$  relation obtained by plotting the mean amplitude of  $i_K$  at the different test potentials tested.  $i_K$  reverses at  $V = -75$  mV and  $\gamma_K = 14$  pS. Intrapipette solution (in mM): 145 NaCl, 5.5 KCl, 2 CaCl<sub>2</sub>, 2 MgCl<sub>2</sub>, 10 HEPES. Adapted from Koren G, Liman ER, Logothetis DE *et al.* (1990) Gating mechanism of a cloned potassium channel expressed in frog oocytes and mammalian cells. *Neuron* 2, 39–51, with permission.

(Figure 4.20b), the macroscopic outward current obtained has a slow time to peak (4 ms) and lasts the entire depolarizing step. It closely resembles the whole cell current recorded with two electrode voltage clamps in the same preparation (rat brain delayed rectifier channels expressed in oocytes; see Figure 4.22a). The whole-cell current amplitude at steady state (once it has reached its maximal amplitude) for a given potential is:

$$I_K = Np_o i_K$$

where  $N$  is the number of delayed rectifier channels in the membrane recorded,  $p_o$  the open probability at steady state and  $i_K$  the elementary current. The number of open channels  $Np_o$  increases with depolarization (to a maximal value) and so does  $I_K$ .

The  $I_K/V$  relation shows that the whole cell current varies linearly with voltage from a threshold potential

which in this preparation is around -40 mV (Figure 4.22b). When the membrane is more hyperpolarized than the threshold potential, very few channels are open and  $I_K$  is equal to zero. For membrane potentials more depolarized than the threshold potential,  $I_K$  depends on  $p_o$  and the driving force state ( $V - E_K$ ) which augments with depolarization. Once  $p_o$  is maximal,  $I_K$  augments linearly with depolarization since it depends only on the driving force.

*The delayed rectifier channels are selective to K<sup>+</sup> ions*

Ion substitution experiments indicate that the reversal potential of  $I_K$  depends on the external K<sup>+</sup> ions concentration as expected for a selective K<sup>+</sup> channel. The reversal potential of the whole cell current is measured as in Figure 4.22b in the presence of different external

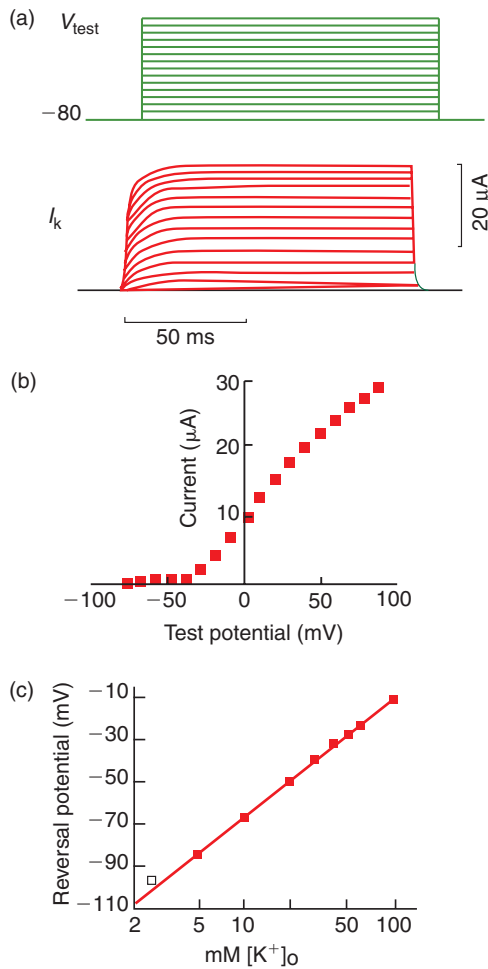


**FIGURE 4.22** Characteristics of the macroscopic delayed rectifier  $K^+$  current.

The activity of  $N$  delayed rectifier channels expressed from rat brain cDNA in oocytes recorded in double-electrode voltage clamp. (a) In response to depolarizing steps of increasing amplitude (given every 2 s) from a holding potential of  $-80$  mV (upper traces), a non-inactivating outward current of increasing amplitude is recorded (lower traces). (b) The amplitude of the current at steady state is plotted against test potential. The potential threshold for its activation is  $-40$  mV. (c) The value of the reversal potentials of the macroscopic current is plotted against the extracellular concentration of  $K^+$  ions on a semi-logarithmic scale. The slope is  $-55$  mV. From Stühmer W, Stocker M, Sakmann B *et al.* (1988) Potassium channels expressed from rat brain cDNA have delayed rectifier properties. *FEBS Lett.* **242**, 199–206, with permission.

concentrations of  $K^+$  ions. These experimental values are plotted against the external  $K^+$  concentration,  $[K^+]_o$ , on a semi-logarithmic scale. For concentrations ranging from 2.5 (normal frog Ringer) to 100 mM, a linear relation with a slope of 55 mV for a 10-fold change in  $[K^+]_o$  is obtained (not shown). These data are well fitted by the Nernst equation. It indicates that the channel has a higher selectivity for  $K^+$  ions over  $Na^+$  and  $Cl^-$  ions.

The delayed rectifier channels are blocked by millimolar concentrations of tetraethylammonium (TEA) and by  $Cs^+$  ions. Ammonium ions can pass through most  $K^+$  channels, whereas its quaternary derivative TEA cannot, resulting in the blockade of most of the voltage-gated  $K^+$  channels: TEA is a small open channel blocker. Amino acids in the carboxyl half of the region linking segments S5 and S6 (i.e. adjacent to S6) influence the sensitivity to pore blockers such as TEA.

#### 4.3.6 Conclusion: during an action potential the consequence of the delayed opening of $K^+$ channels is an exit of $K^+$ ions, which repolarizes the membrane to resting potential

Owing to their delay of opening, delayed rectifier channels open when the membrane is already depolarized by the entry of  $Na^+$  ions through open voltage-gated  $Na^+$  channels (Figure 4.23). Therefore, the exit of  $K^+$  ions does not occur at the same time as the entry of  $Na^+$  ions (see also Figure 4.24). This allows the membrane to first depolarize in response to the entry of  $Na^+$  ions and then to repolarize as a consequence of the exit of  $K^+$  ions.

### 4.4 SODIUM-DEPENDENT ACTION POTENTIALS ARE INITIATED AT THE AXON INITIAL SEGMENT IN RESPONSE TO A MEMBRANE DEPOLARIZATION AND THEN ACTIVELY PROPAGATE ALONG THE AXON

$Na^+$ -dependent action potentials, because of their short duration (1–5 ms), are also named spikes.  $Na^+$  spikes, for a given cell, have a stable amplitude and duration; they all look alike, and are binary, all-or-none. The pattern of discharge (which is often different from the frequency of discharge) and not individual spikes, carries significant information.

#### 4.4.1 Summary on the $Na^+$ -dependent action potential

The depolarization phase of  $Na^+$  spikes is due to the rapid time to peak inward  $Na^+$  current which flows into the axon initial segment or node. This depolarization is brief because the inward  $Na^+$  current inactivates in milliseconds (Figure 4.24b).

In the squid giant axon or frog axon, spike repolarization is associated with an outward  $K^+$  current

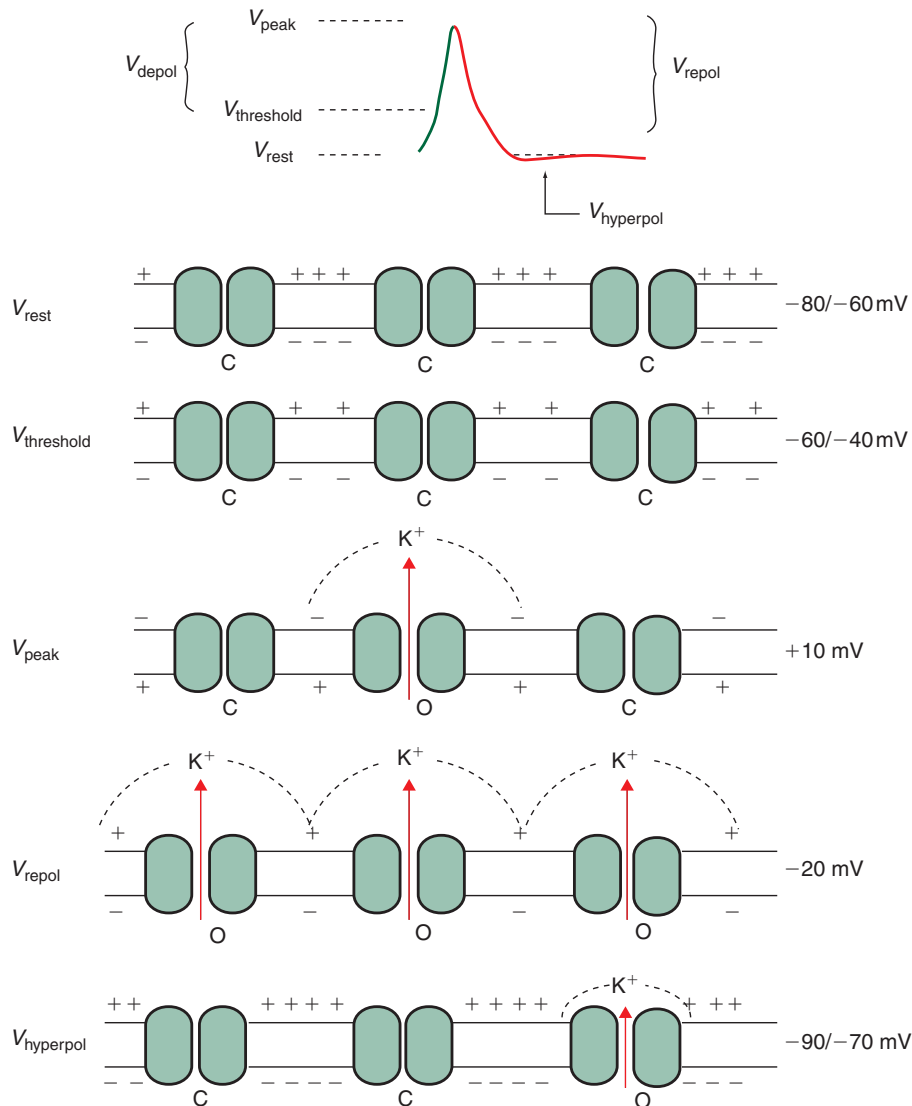


FIGURE 4.23 States of the delayed rectifier  $\text{K}^+$  channels in relation to the different phases of the  $\text{Na}^+$ -dependent action potential.

C, closed state; O, open state;  $\uparrow$ , driving force for  $\text{K}^+$  ions.

through delayed rectifier channels (Figures 4.24 and 4.25) since TEA application dramatically prolongs the action potential (see Figure 4.4b). As pointed out by Hodgkin and Huxley: 'The rapid rise is due almost entirely to  $\text{Na}^+$  conductance, but after the peak, the  $\text{K}^+$  conductance takes a progressively larger share until, by the beginning of the hyperpolarized phase, the  $\text{Na}^+$  conductance has become negligible. The tail of raised conductance that falls away gradually during the positive phase is due solely to  $\text{K}^+$  conductance, the small constant leak conductance being of course present throughout.'

In contrast, in rat or rabbit myelinated axons the action potential is very little affected by the application of TEA. The repolarization phase in these preparations is largely associated with a leak  $\text{K}^+$  current. Voltage

clamp studies confirm this observation. When the leak current is subtracted, almost no outward current is recorded in rabbit node (Figure 4.25b).

However, squid and rabbit nerve action potentials have the same duration (Figure 4.25a). In this preparation, the normal resting membrane potential is around  $-80\text{ mV}$ , which suggests the presence of a large leak  $\text{K}^+$  current. Moreover, test depolarizations evoke large outward  $\text{K}^+$  currents insensitive to TEA (Figure 4.26). How does the action potential repolarize in such preparations? First the  $\text{Na}^+$  currents in the rabbit node inactivate two to three times faster than those in the frog node. Second, the large leak  $\text{K}^+$  current present at depolarized membrane potentials repolarizes the membrane. The amplitude of the leak  $\text{K}^+$  current augments linearly with depolarization, depending only on the  $\text{K}^+$  driving force.

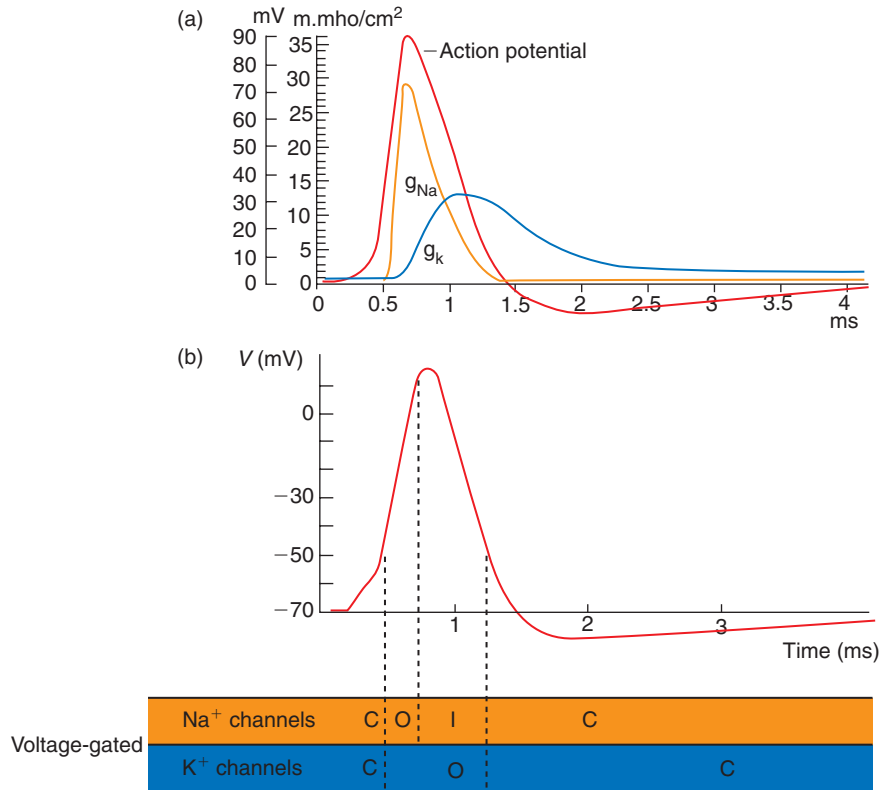


**FIGURE 4.24** Gating of Na<sup>+</sup> and K<sup>+</sup> channels during the Na<sup>+</sup>-dependent action potential. (a) Interpretation of the manner in which the conductances to Na<sup>+</sup> and K<sup>+</sup> contribute to the action potential. (b) State of the Na<sup>+</sup> and K<sup>+</sup> voltage-gated channels during the course of the action potential. O, channels open; I, channels inactivate; C, channels close or are closed. Trace (a) adapted from Hodgkin AL and Huxley AF (1952) A quantitative description of membrane current and its application to conduction and excitation in nerve. *J. Physiol.* 117, 500–544, with permission.

#### 4.4.2 Depolarization of the membrane to the threshold for voltage-gated Na<sup>+</sup> channel activation has two origins

The inward current which depolarizes the membrane of the initial segment to the threshold potential for voltage-gated Na<sup>+</sup> channel opening is one of the following:

- A depolarizing current resulting from the activity of excitatory afferent synapses (see Chapters 8 and 10) or afferent sensory stimuli. In the first case, the synaptic currents generated at postsynaptic sites in response to synaptic activity summate, and when the resulting current is inward it can depolarize the membrane to the threshold for spike initiation. In the second case, sensory stimuli are transduced in inward currents that can depolarize the membrane to the threshold for spike initiation.
- An intrinsic regenerative depolarizing current such as, for example, in heart cells or invertebrate neurons.

#### 4.4.3 The site of initiation of Na<sup>+</sup>-dependent action potentials is the axon initial segment

The site of initiation was suggested long ago to occur in the axon initial segment since the threshold for spike initiation was the lowest at this level. However, this has only recently been directly demonstrated with the double-patch clamp technique. First the dendrites and soma belonging to the same Purkinje neuron of the cerebellum are visualized in a rat brain slice. Then the activity is recorded simultaneously at both these sites with two patch electrodes (whole-cell patches). To verify that somatic and dendritic recordings are made from the same cell, the Purkinje cell is filled with two differently coloured fluorescent dyes: Cascade blue at the soma and Lucifer yellow at the dendrite. To determine the site of action potential initiation during synaptic activation of Purkinje cells, action potentials are evoked by stimulation of afferent parallel fibres which make synapses on distal dendrites of Purkinje cells (see **Figures 6.8** and **6.9**).

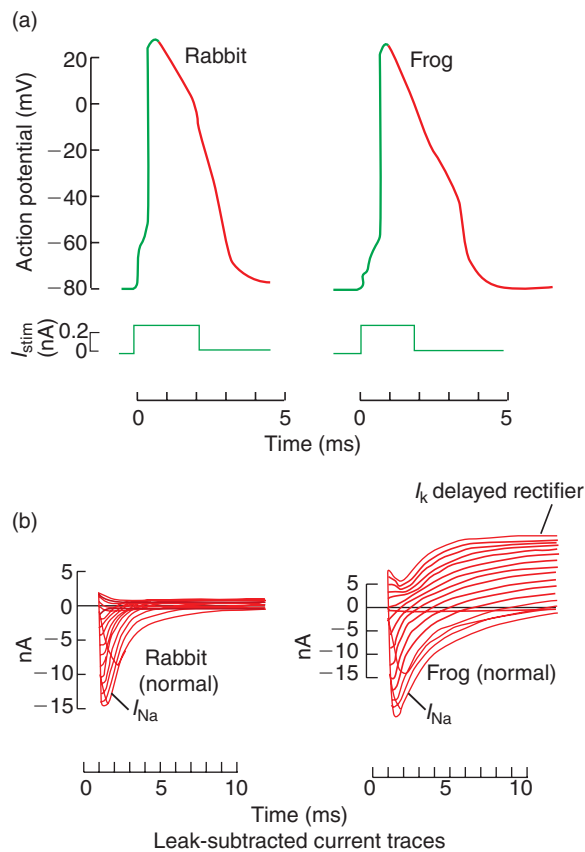


**FIGURE 4.25** The currents underlying the action potentials of the rabbit and frog nerves.

(a) The action potentials are recorded intracellularly at  $14^\circ\text{C}$ . Bottom trace is the current of stimulation injected in order to depolarize the membrane to initiate an action potential. (b) The currents flowing through the membrane at different voltages recorded in voltage clamp. In the rabbit node, very little outward current is recorded after the large inward  $\text{Na}^+$  current. In the frog nerve, a large outward  $\text{K}^+$  current is recorded after the large inward  $\text{Na}^+$  current. Leak current is subtracted from each trace and does not appear in these recordings. Adapted from Chiu SY, Ritchie JM, Bogart RB, Stagg D (1979) A quantitative description of membrane currents in rabbit myelinated nerve. *J. Physiol.* 292, 149–166, with permission.

In all Purkinje cells tested, the evoked action potential recorded from the soma has a shorter delay and a greater amplitude than that recorded from a dendrite (Figure 4.27a). Moreover, the delay and the difference in amplitude between the somatic spike and the dendritic spike both augment when the distance between the two patch electrodes is increased. This suggests that the site of initiation is proximal to the soma.

Simultaneous whole-cell recordings from the soma and the axon initial segment were performed to establish whether action potential initiation is somatic or axonal in origin. Action potentials clearly occurs first in the axon initial segment (Figure 4.27b). These

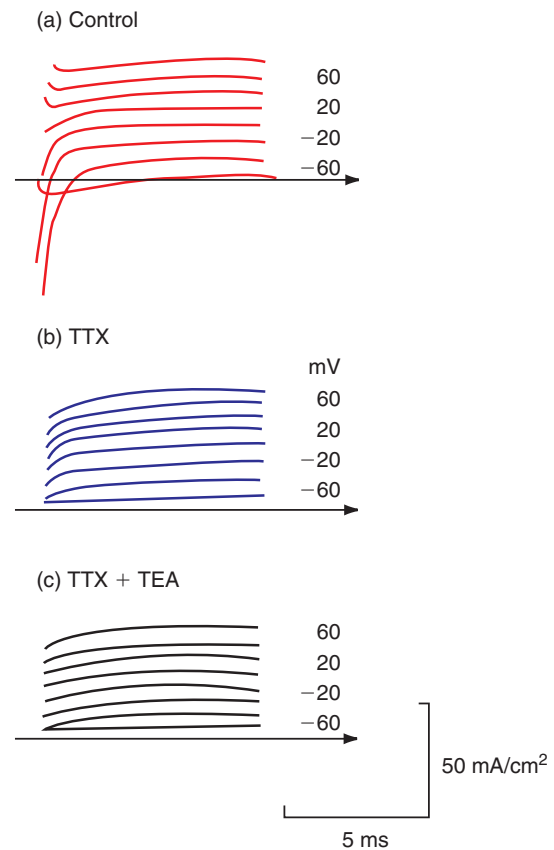


**FIGURE 4.26** TEA-resistant outward current in a mammalian nerve.

The currents evoked by depolarizing steps from  $-60$  to  $+60$  mV from a holding potential of  $-80$  mV are recorded in voltage clamp in a node of Ranvier of an isolated rat nerve fibre. Control inward and outward currents (a), after TTX 25 nM (b), and after TTX 25 nM and TEA 5 mM (c) are added to the extracellular solution. The outward current recorded in (c) is the leak  $\text{K}^+$  current. The delayed outward  $\text{K}^+$  current is taken as the difference between the steady-state outward current in (b) and the leak current in (c). Adapted from Brismar T (1980) Potential clamp analysis of membrane currents in rat myelinated nerve fibres. *J. Physiol.* 298, 171–184, with permission.

results suggest that the actual site of  $\text{Na}^+$ -dependent action potential initiation is in the axon initial segment of Purkinje cells. Experiments carried out by Sakmann *et al.* in other brain regions give the same conclusion for all the neurons tested. This may be due to a higher density of sodium channels in the membrane of the axon initial segment.

The action potential, once initiated, spreads passively back into the dendritic tree of Purkinje cells (passively means that it propagates with attenuation since it is not reinitiated in dendrites). Simultaneously it actively propagates into the axon (not shown here; see below). In some neurons, for example the pyramidal cells of the neocortex, the action potential actively

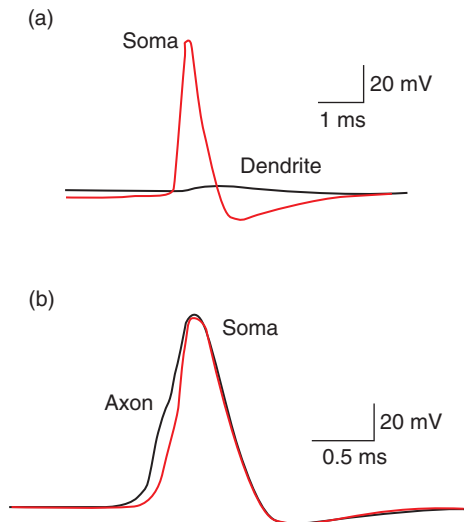


**FIGURE 4.27** The  $\text{Na}^+$ -dependent action potential is initiated in the axon initial segment in Purkinje cells of the cerebellum.

The activity of a Purkinje cell recorded simultaneously at the level of the soma and (a) 117  $\mu\text{m}$  away from the soma at the level of a dendrite, or (b) 7  $\mu\text{m}$  away from the soma at the level of the axon initial segment, with the double-patch clamp technique (whole-cell patches). Afferent parallel fibres are stimulated by applying brief voltage pulses to an extracellular patch pipette. In response to the synaptic excitation, an action potential is evoked in the Purkinje cell and recorded at the two different neuronal sites: soma and dendrite (a) or soma and axon (b). Adapted from Stuart G and Hauser M (1994) Initiation and spread of sodium action potentials in cerebellar Purkinje cells. *Neuron* 13, 703–712, with permission.

backpropagates into the dendrites, but this is not a general rule.

#### 4.4.4 The $\text{Na}^+$ -dependent action potential actively propagates along the axon to axon terminals

Voltage-gated  $\text{Na}^+$  channels are present all along the axon at a sufficient density to allow firing of axon potentials.

##### *The propagation is active*

Active means that the action potential is reinitiated at each node of Ranvier for a myelinated axon, or at each point for a non-myelinated axon. The flow of  $\text{Na}^+$  ions through the open  $\text{Na}^+$  voltage-gated channels of the axon initial segment creates a current that spreads passively along the length of the axon to the first node of Ranvier (Figure 4.28). It depolarizes the membrane of the first node to the threshold for action potential initiation. The action potential is now at the level of the

first node. The entry of  $\text{Na}^+$  ions at this level will depolarize the membrane of the second node and open the closed  $\text{Na}^+$  channels. The action potential is now at the level of the second node.

##### *The propagation is unidirectional owing to $\text{Na}^+$ channel inactivation*

When the axon potential is, for example, at the level of the second node, the voltage-gated  $\text{Na}^+$  channels of the first node are in the inactivated state since they have just been activated or are still in the open state (Figure 4.28). These  $\text{Na}^+$  channels cannot be reactivated. The current lines flowing from the second node will therefore activate only the voltage-gated  $\text{Na}^+$  channels of the third node towards axon terminals, where the voltage-gated  $\text{Na}^+$  channels are in the closed state (Figure 4.28). In the axon, under physiological conditions, the action potential cannot back-propagate.

##### *The refractory periods between two action potentials*

After one action potential has been initiated, there is a period of time during which a second action potential cannot be initiated or is initiated but has a smaller amplitude (Figure 4.29): this period is called the ‘refractory period’ of the membrane. It results from  $\text{Na}^+$  channel inactivation. Since the  $\text{Na}^+$  channels do not immediately recover from inactivation, they cannot reopen immediately. This means that once the preceding action potential has reached its maximum amplitude,  $\text{Na}^+$  channels will not reopen before a certain period of time needed for their deinactivation (Figure 4.24b). This represents the absolute refractory period which lasts in the order of milliseconds.

Then, progressively, the  $\text{Na}^+$  channels will recover from inactivation and some will reopen in response to a second depolarization: this is the relative refractory period. This period finishes when all the  $\text{Na}^+$  channel at the initial axonal segment or at a node are de-inactivated. This actually protects the membrane from being depolarized all the time and enables the initiation of separate action potentials.

#### 4.4.5 Do the $\text{Na}^+$ and $\text{K}^+$ concentrations change in the extracellular or intracellular media during firing?

Over a short timescale, the external or internal  $\text{Na}^+$  or  $\text{K}^+$  concentrations do not change during the emission

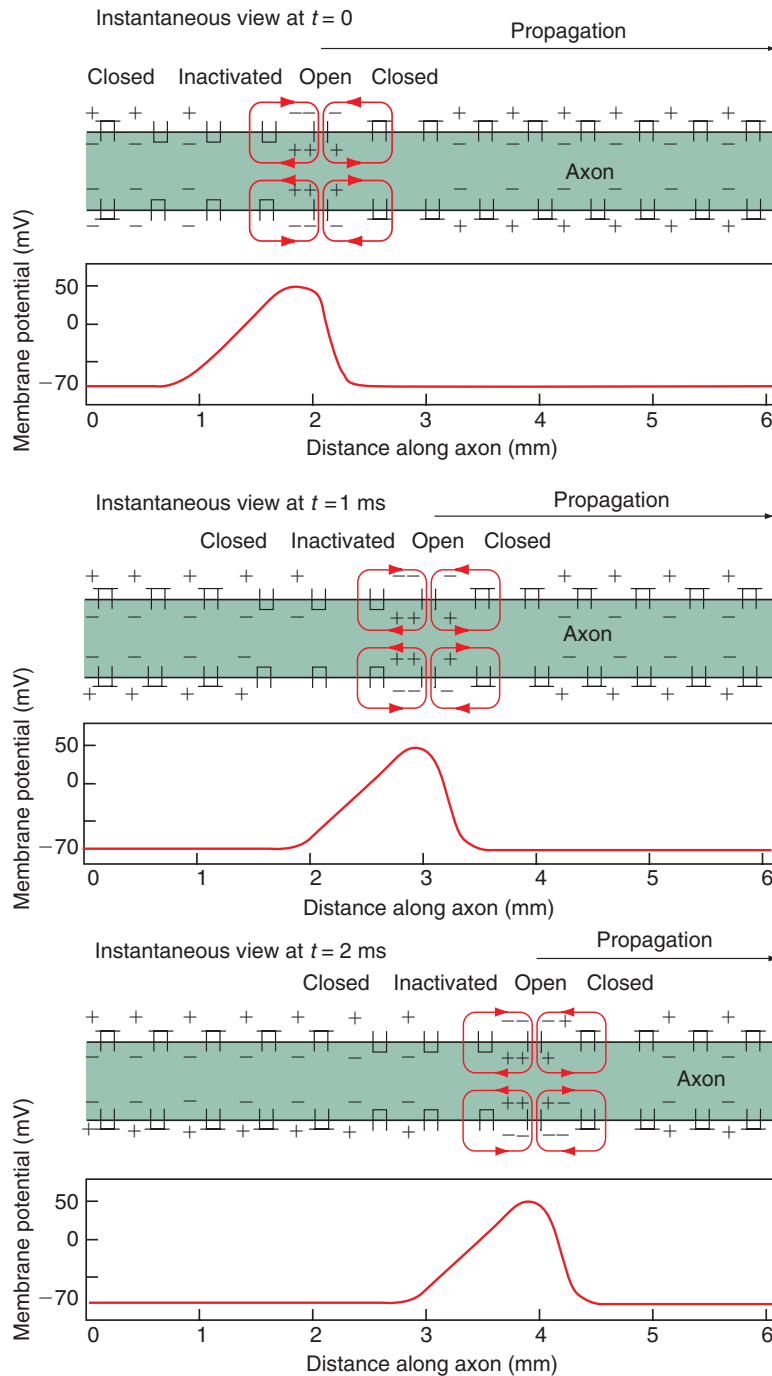
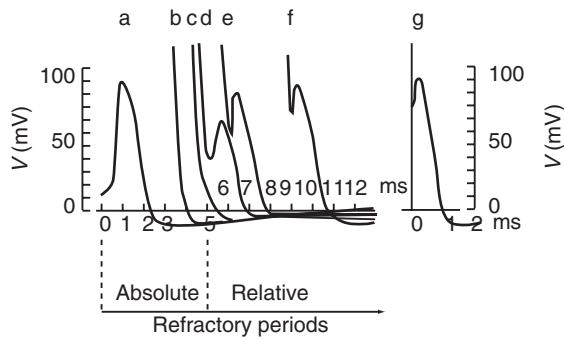


FIGURE 4.28 Active propagation of the  $\text{Na}^+$ -dependent action potential in the axon and axon collaterals. Scheme provided by Alberts B, Bray D, Lewis J *et al.* (1983) *Molecular Biology of the Cell*, New York: Garland Publishing.

of action potentials. A small number of ions are in fact flowing through the channels during an action potential and the Na–K pump re-establishes continuously the extracellular and intracellular  $\text{Na}^+$  and  $\text{K}^+$  concentrations at the expense of ATP hydrolysis. Over a longer timescale, during high-frequency trains of action

potentials, the  $\text{K}^+$  concentration can significantly increase in the external medium. This is due to the very small volume of the extracellular medium surrounding neurons and the limited speed of the Na–K pump. This excess of  $\text{K}^+$  ions is buffered by glial cells which are highly permeable to  $\text{K}^+$  ions (see Section 2.1.3).



**FIGURE 4.29** The refractory periods.

A first action potential is recorded intracellularly in the squid axon *in vitro* in response to a small depolarizing stimulus (a). Then a second stimulus with an intensity six times greater than that of the first is applied 4, 5, 6 or 9 ms after. The evoked spike is either absent (b and c; only the stimulation artifact is recorded) or has a smaller amplitude (d to f). Finally, when the membrane is back in the resting state, the evoked action potential has the control amplitude (g). Adapted from Hodgkin AL and Huxley AF (1952) A quantitative description of membrane current and its application to conduction and excitation in nerve. *J. Physiol.* **117**, 500–544, with permission.

#### 4.4.6 Characteristics of the Na<sup>+</sup>-dependent action potential are explained by the properties of the voltage-gated Na<sup>+</sup> channel

The *threshold* for Na<sup>+</sup>-dependent action potential initiation results from the fact that voltage-gated Na<sup>+</sup> channels open in response to a depolarization positive to  $-50/-40$  mV.

The Na<sup>+</sup>-dependent action potential is *all or none* because voltage-gated Na<sup>+</sup> channels self-activate (see **Figure 4.17**). It propagates *without attenuation* since the density of voltage-gated Na<sup>+</sup> channels is constant along the axon or at nodes of Ranvier. It propagates *unidirectionally* because of the rapid inactivation of voltage-gated Na<sup>+</sup> channels. The instantaneous frequency of Na<sup>+</sup>-dependent action potentials is limited by the *refractory periods*, which also results from voltage-gated Na<sup>+</sup> channel inactivation.

#### 4.4.7 The role of the Na<sup>+</sup>-dependent action potential is to evoke neurotransmitter release

The role of the Na<sup>+</sup>-dependent action potential is to propagate, without attenuation, a strong depolarization to the membrane of the axon terminals. There, this depolarization opens the high-threshold voltage-gated

Ca<sup>2+</sup> channels. The resulting entry of Ca<sup>2+</sup> ions into axon terminals triggers exocytosis and neurotransmitter release. The probability value of all these phenomena is not 1. This means that the action potential can fail to invade an axon terminal, the Ca<sup>2+</sup> entry can fail to trigger exocytosis, etc. Neurotransmitter release is explained in Chapter 7.

### FURTHER READING

- Anderson PAV and Greenberg RM (2001) Phylogeny of ion channels: clues to structure and function. *Comparative Biochemistry and Physiology Part B* **129**, 17–28.
- Catterall WA (2000) From ionic currents to molecular mechanisms: the structure and function of voltage-gated sodium channels. *Neuron* **26**, 13–25.
- Eaholtz G, Scheuer T, Catterall WA (1994) Restoration of inactivation and block of open sodium channels by an inactivation gate peptide. *Neuron* **12**, 1041–1048.
- Goldin AL, Barchi RL, Caldwell JH *et al.* (2000) Nomenclature of voltage-gated sodium channels. *Neuron* **28**, 365–368.
- Hamill OP, Marty A, Neher E *et al.* (1981) Improved patch clamp technique for high resolution current recording from cells and cell-free membrane patches. *Pflügers Archiv*. **391**, 85–100.
- Hodgkin AL and Huxley AF (1952) A quantitative description of membrane current and its application to conduction and excitation in nerve. *J. Physiol. (Lond.)* **117**, 500–544.
- Malin SA, Nerbonne JM (2002) delayed rectifier K<sup>+</sup> currents,  $I_{Kv}$ , are encoded by Kv2  $\alpha$ -subunits and regulate tonic firing in mammalian sympathetic neurons. *J. Neuroscience* **22**, 10094–10105.
- McCormick KA, Srinivasan J, White K, Scheuer T, Catterall WA (1999) The extracellular domain of the beta1 subunit is both necessary and sufficient for beta1-like modulation of sodium channel gating. *J. Biol. Chem.* **274**, 32638–32646.
- McKinnon R (2003) Potassium channels. *FEBS Letters* **555**, 62–65.
- Neher E, Sakmann B (1976) Single channel currents recorded from membrane of denervated frog muscle fibres. *Nature* **260**, 779–802.
- Noda M, Ikeda T, Suzuki H *et al.* (1986) Expression of functional sodium channels from cloned cDNA. *Nature* **322**, 826–828.
- Qu Y, Rogers JC, Chen SF, McCormick KA, Scheuer T, Catterall WA (1999) Functional roles of the extracellular segments of the sodium channel alpha subunit in voltage-dependent gating and modulation by beta1 subunits. *J. Biol. Chem.* **274**, 32647–32654.
- Sokolov S, Scheuer T, Catterall WA (2005) Ion permeation through a voltage-sensitive gating pore in brain sodium channels having voltage sensor mutations. *Neuron* **47**, 183–189.
- Stuart G and Häuser M (1994) Initiation and spread of sodium action potentials in cerebellar Purkinje cells. *Neuron* **13**, 703–712.
- Vassilev PM, Scheuer T, Catterall WA (1988) Identification of an intracellular peptide segment involved in sodium channel inactivation. *Science* **241**, 1658–1661.
- Venkatesh B, Lu SQ, Dandona N *et al.* (2005) Genetic basis of tetrodotoxin resistance in pufferfishes. *Current Biology* **15**, 2069–2072.
- Wang SY and Wang GK (2003) Voltage-gated sodium channels as primary targets of diverse lipid soluble neurotoxins. *Cellular Signaling* **15**, 151–159.

## APPENDIX 4.1 CURRENT CLAMP RECORDING

The current clamp technique, or intracellular recording in current clamp mode, is the traditional method for recording membrane potential: resting membrane potential and membrane potential changes such as action potentials and postsynaptic potentials. Membrane potential changes result from intrinsic or extrinsic currents. Intrinsic currents are synaptic or autorhythmic currents. Extrinsic currents are currents of known amplitude and duration applied by the experimenter through the intracellular recording electrode, in order to mimic currents produced by synaptic inputs.

Current clamp means that the *current applied* through the intracellular electrode is clamped to a constant value by the experimenter. It does not mean that the *current flowing through the membrane* is clamped to a constant value.

### How to record membrane potential

The intracellular electrode (or the patch pipette) is connected to a unity-gain amplifier that has an input resistance many orders of magnitude greater than that of the micropipette plus the input resistance of the cell membrane ( $R_p + R_m$ ). The output of the amplifier follows the voltage at the tip of the intracellular electrode ( $V_p$ ) (**Figure A4.1**). By definition, membrane potential  $V_m$  is equal to  $V_i - V_e$  (i for intracellular and e for extracellular). In **Figure A4.1**,  $V_i - V_e = V_p - V_{\text{bath}} = V_p - V_{\text{ground}} = V_p - 0 = V_p$ . When a current  $I$  is simultaneously passed through the electrode,  $V_p = V_m$  as

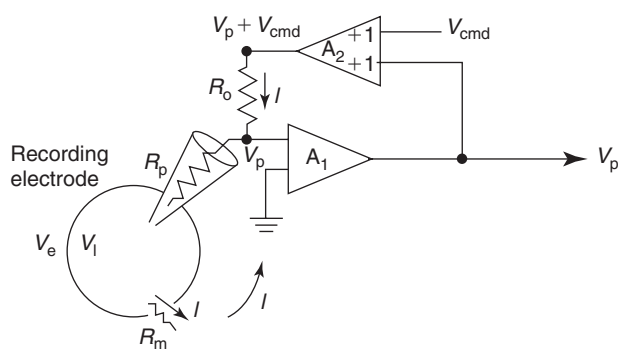


**FIGURE A4.1** A unity gain amplifier A1 and a current source made by adding a second amplifier A2.

The micropipette voltage  $V_p$  is measured by A1. The command voltage  $V_{\text{cmd}}$  and  $V_p$  are the inputs of A2 ( $V_p$  and  $V_{\text{cmd}}$  are added). The current  $I$  applied by the experimenter in order to induce  $V_m$  changes, flows through  $R_o$  and is equal to  $I = V_p/R_o$  since the voltage across the output resistor  $R_o$  is equal to  $V_{\text{cmd}}$  regardless of  $V_p$ .  $I$  flows through the micropipette into the cell then out through the cell membrane into the bath grounding electrode.  $I$  is here an outward current. Capacitances are ignored. Adapted from *The Axon Guide*, Axon Instruments Inc., 1993.

long as the current  $I$  is very small in order not to cause a significant voltage drop across  $R_p$  (see the last section of this appendix).

### How to inject current through the intracellular electrode

In a current injection circuit is connected to the input node, the current injected ( $I$ ) flows down the electrode into the cell (**Figure A4.1**). This current source allows a constant (DC) current to be injected, either outward to depolarize the membrane or inward to hyperpolarize the membrane (**Figure A4.2**). When the recording electrode is filled with KCl, a current that expels  $\text{K}^+$  ions into the cell interior depolarizes the membrane ( $V_m$  becomes less negative) (**Figure A4.2a**), whereas a current that expels  $\text{Cl}^-$  ions into the cell interior hyperpolarizes the membrane ( $V_m$  becomes more negative) (**Figure A4.2b**).

*Outward means that the current is flowing through the membrane from the inside of the cell to the bath; inward is the opposite*

The current source can also be used to inject a short-duration pulse of current: a depolarizing current pulse above threshold to evoke action potential(s) or a low-amplitude depolarizing (**Figure A4.3**) or hyperpolarizing

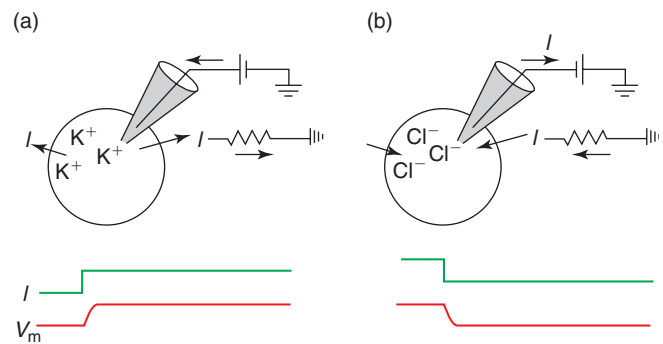


**FIGURE A4.2** (a) When the recording electrode is filled with KCl, a current expels  $\text{K}^+$  ions into the cell interior to depolarize the membrane ( $V_m$  becomes less negative). (b) A current expels  $\text{Cl}^-$  ions into the cell interior to hyperpolarize the membrane ( $V_m$  becomes more negative).

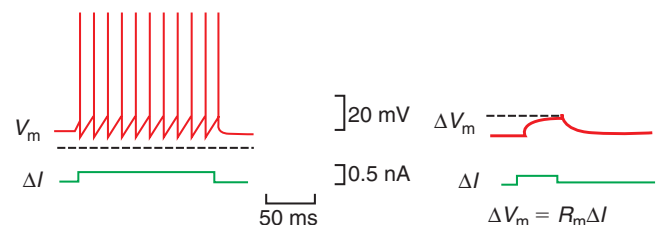


**FIGURE A4.3** Injection of a suprathreshold (left) and subthreshold (right) depolarizing pulse.

current pulse to measure the input membrane resistance  $R_m$  since  $\Delta V_m = R_m \times \Delta I$ .

*How to measure the membrane potential when a current is passed down the electrode*

The injected current ( $I$ ) causes a corresponding voltage drop ( $IR_p$ ) across the resistance of the pipette ( $R_p$ ). It is therefore difficult to separate the potential at the tip of the electrode ( $V_p = V_m$ ) from the total potential ( $V_p + IR_p$ ). For example, if  $R_p = 50 \text{ M}\Omega$  and  $I = 0.5 \text{ nA}$ ,  $IR_p = 25 \text{ mV}$ , a value in the  $V_m$  range. A special compensation circuitry can be used to eliminate the micropipette voltage drop  $IR_p$ .

## APPENDIX 4.2 VOLTAGE CLAMP RECORDING

The voltage clamp technique (or intracellular recording in voltage clamp mode) is a method for recording the current flowing through the cell membrane while the membrane potential is held (clamped) at a constant value by the experimenter. In contrast to the current clamp technique (see Appendix 4.1), voltage clamp does not mimic a process found in nature. However, there are several reasons for performing voltage clamp experiments:

- When studying voltage-gated channels, voltage clamp allows control of a variable (voltage) that determines the opening and closing of these channels.
- By holding the membrane potential constant, the experimenter ensures that the current flowing through the membrane is linearly proportional to the conductance  $G$  ( $G = 1/R$ ) being studied. To study, for example, the conductance  $G_{\text{Na}}$  of the total number ( $N$ ) of voltage-gated  $\text{Na}^+$  channels present in the membrane,  $\text{K}^+$  and  $\text{Ca}^{2+}$  voltage-gated channels are blocked by pharmacological agents, and the current  $I_{\text{Na}}$  flowing through the membrane, recorded in voltage clamp, is proportional to  $G_{\text{Na}}$ :

$$I_{\text{Na}} = V_m G_{\text{Na}} = k G_{\text{Na}}, \text{ since } V_m \text{ is constant.}$$

*How to clamp the membrane potential at a known and constant value*

The aim of the voltage clamp technique is to adjust continuously the membrane potential  $V_m$  to the command potential  $V_{\text{cmd}}$  fixed by the experimenter. To do so,  $V_m$  is continuously measured *and* a current  $I$  is passed through the cell membrane to keep  $V_m$  at the desired

value or command potential ( $V_{\text{cmd}}$ ). Two voltage clamp techniques are commonly used. With the two-electrode voltage clamp method, one electrode is used for membrane potential measurement and the other for passing current (**Figure A4.4**). The other method uses just one electrode, in one of the following ways:

- The same electrode is used part time for membrane potential measurement and part time for current injection (also called the discontinuous single-electrode voltage clamp technique, or dSEVC). This is used for cells that are too small to be impaled with two electrodes; it will not be explained here.
- In the patch clamp technique the same electrode is used full time for simultaneously measuring membrane potential and passing current (see Appendix 4.3).

In the two-electrode voltage clamp technique, the membrane potential is recorded by a unity gain amplifier A1 connected to the voltage-recording electrode E1. The membrane potential measured,  $V_m$  (or  $V_p$ ; see Appendix 4.1) is compared with the command potential  $V_{\text{cmd}}$  in a high-gain differential amplifier A2. It sends a voltage output  $V_o$  proportional to the difference between  $V_m$  and  $V_{\text{cmd}}$ .  $V_o$  forces a current  $I$  to flow through the current-passing electrode E2 in order to obtain  $V_m - V_{\text{cmd}} = 0$ . The current  $I$  represents the total current that flows through the membrane. It is the same at every point of the circuit.

*Example of a voltage-clamp recording experiment*

Two electrodes are placed intracellularly into a neuronal soma (an invertebrate neuron for example) (**Figure A4.5**). The membrane potential is first held at  $-80 \text{ mV}$ . In this condition an outward current flows

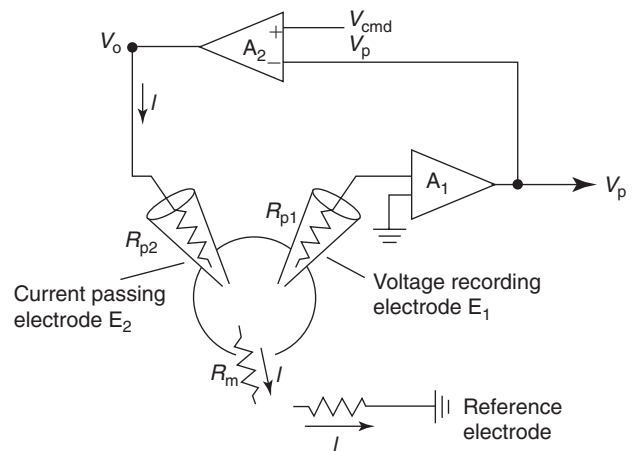


**FIGURE A4.4 Two-electrode voltage clamp.**

Adapted from *The Axon Guide*, Axon Instruments Inc., 1993.

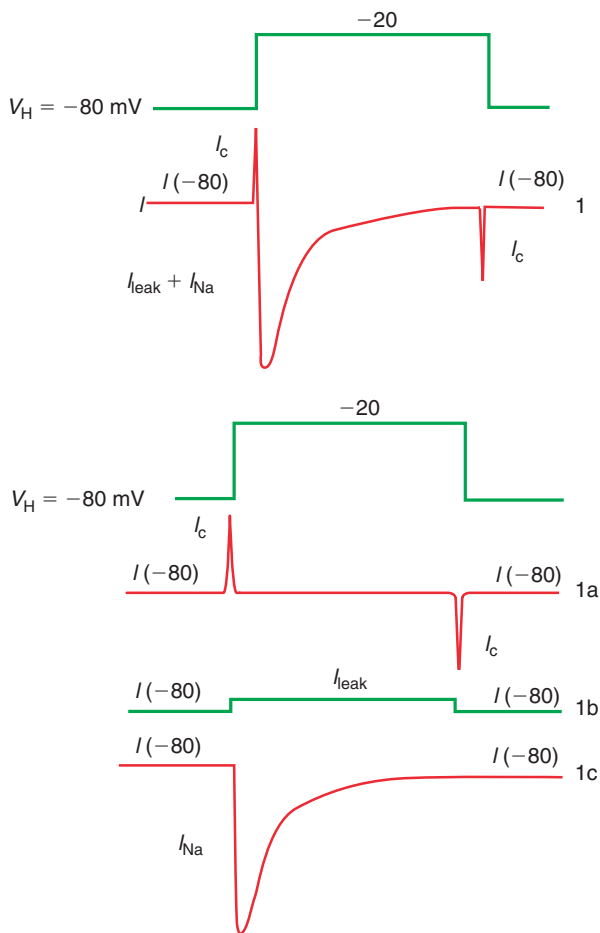


FIGURE A4.5 Various currents.

(1 = 1a + 1b + 1c) evoked by a voltage step to  $-20$  mV ( $V_H = -80$  mV) in the presence of  $\text{K}^+$  and  $\text{Ca}^{2+}$  channel blockers.

through the membrane in order to maintain the membrane potential at a value more hyperpolarized than  $V_{\text{rest}}$ . This stable outward current  $I_{-80}$  flows through the membrane as long as  $V_{\text{cmd}} = -80$  mV.

A voltage step to  $-20$  mV is then applied for 100 ms. This depolarizing step opens voltage-gated channels. In the presence of  $\text{K}^+$  and  $\text{Ca}^{2+}$  channel blockers, only a voltage-gated  $\text{Na}^+$  current is recorded. To clamp the membrane at the new  $V_{\text{cmd}} = -20$  mV, a current  $I_{(-20)}$  is sent by the amplifier A2. On the rising phase of the step this current is equal to the capacitive current  $I_c$  necessary to charge the membrane capacitance to its new value plus the leak current  $I_L$  flowing through leak channels (lines 1a and 1b). Since the depolarizing step opens  $\text{Na}^+$  voltage-gated channels, an inward current  $I_{\text{Na}}$  flowing through open  $\text{Na}^+$  channels will appear after a small delay (line 1c). Normally, this inward current flowing through the open  $\text{Na}^+$  channels,  $I_{\text{Na}}$ , should depolarize the membrane but in voltage clamp experiments it does not: a current constantly equal to

$I_{\text{Na}}$  but of opposite direction is continuously sent (in the microsecond range) in the circuit to compensate  $I_{\text{Na}}$  and to clamp the membrane to  $V_{\text{cmd}}$ . Therefore, once the membrane capacitance is charged,  $I_{(-20)} = I_L + I_{\text{Na}}$ . Usually on recordings,  $I_c$  is absent owing to the possibility of compensating for it with the voltage clamp amplifier.

Once the membrane capacitance is charged, the total current flowing through the circuit is  $I = I_L + I_{\text{Na}}$  ( $I_c = 0$ ). Therefore, in all measures of  $I_{\text{Na}}$ , the leak current  $I_L$  must be deduced. To do so, small-amplitude hyperpolarizing or depolarizing steps ( $\Delta V_m = \pm 5$  to  $\pm 20$  mV) are applied at the beginning and at the end of the experiment. These voltage steps are too small to open voltage-gated channels in order to have  $I_{\text{Na}} = 0$  and  $I = I_L$ . If we suppose that  $I_L$  is linearly proportional to  $\Delta V_m$ , then  $I_L$  for a  $\Delta V_m$  of  $+80$  mV (from  $-80$  to  $0$  mV) is eight times the value of  $I_L$  for  $\Delta V_m = +10$  mV (see Figure 3.9d).

#### Is all the membrane surface clamped?

In small and round cells such as pituitary cells, the membrane potential is clamped on all the surface. In contrast, in neurons, because of their geometry, the voltage clamp is not achieved on all the membrane surface: the distal dendritic and axonal membranes are out of control because of their distance from the soma where the intracellular electrodes are usually placed. Such space clamp problems have to be taken into account by the experimenter in the analysis of the results. In the giant axon of the squid, this problem is overcome by inserting two long axial intracellular electrodes into a segment of axon in order to control the membrane potential all along this segment.

### APPENDIX 4.3 PATCH CLAMP RECORDING

The patch clamp technique is a variation of the voltage clamp technique. It allows the recording of current flowing through the membrane: either the current flowing through all the channels open in the whole cell membrane or the current flowing through a single channel in a patch of membrane. In this technique, only one electrode is used full time for both voltage recording and passing current (it is a continuous single-electrode voltage clamp technique, or cSEVC). The patch clamp technique was developed by Neher and Sakmann. By applying very low doses of acetylcholine to a patch of muscle membrane they recorded for the first time, in 1976, the current flowing through a single

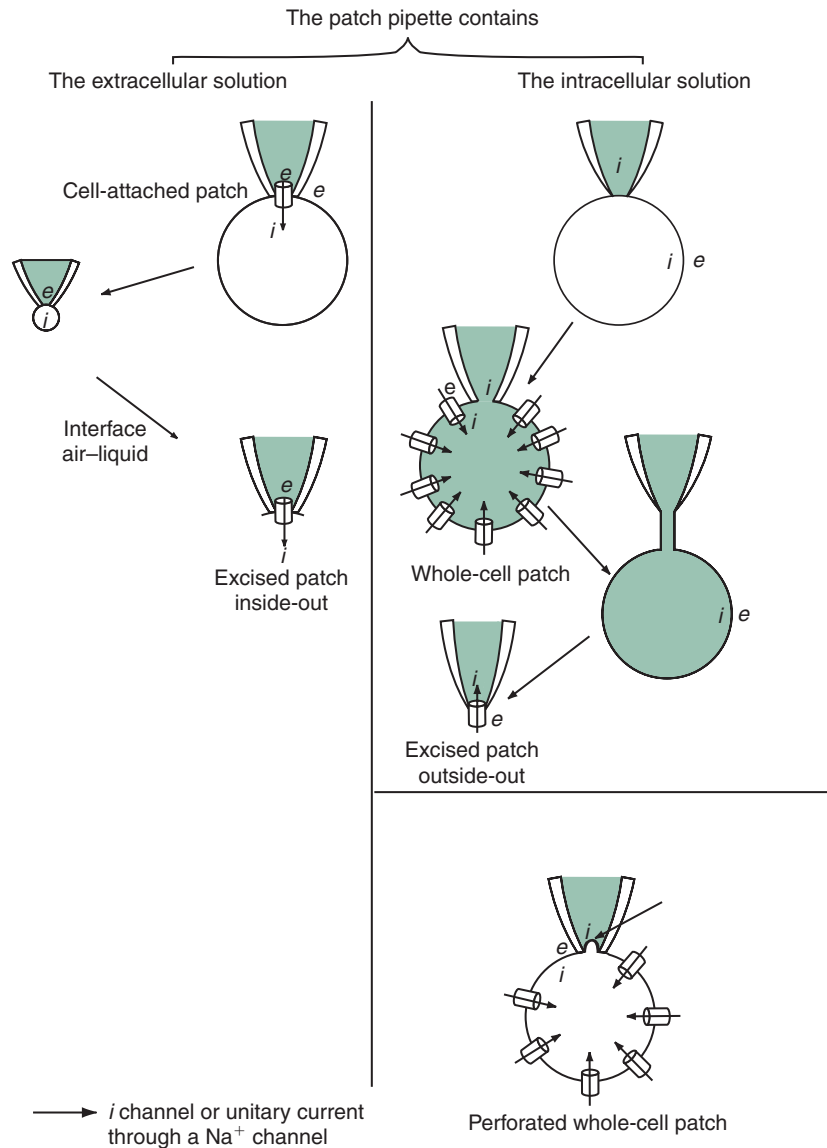


FIGURE A4.6 Configurations of patch clamp recording.

nicotinic cholinergic receptor channel (nAChR), the unitary nicotinic current.

Some of the advantages of the patch clamp technique are that (i) with all but one configuration (cell-attached configuration) the investigator has access to the intracellular environment (Figure A4.6); (ii) it allows the recording of currents from cells too small to be impaled with intracellular microelectrodes; and (iii) it allows the recording of unitary currents (current through a single channel).

#### A4.3.1 The various patch clamp recording configurations

First a tight seal between the membrane and the tip of the pipette must be obtained. The tip of a micropipette

that has been fire polished to a diameter of about  $1\ \mu\text{m}$  is advanced towards a cell until it makes contact with its membrane. Under appropriate conditions, a gentle suction applied to the inside of the pipette causes the formation of a very tight seal between the membrane and the tip of the pipette. This is the cell-attached configuration (Figure A4.6). The resistance between the interior of the pipette and the external solution can be very large, of the order of  $10\ \text{G}\Omega$  ( $10^9\ \Omega$ ) or more. It means that the interior of the pipette is isolated from the extracellular solution by the seal that is formed.

This very large resistance is necessary for two reasons (Figure A4.7):

- It allows the electrical isolation of the membrane patch under the tip of the pipette since practically

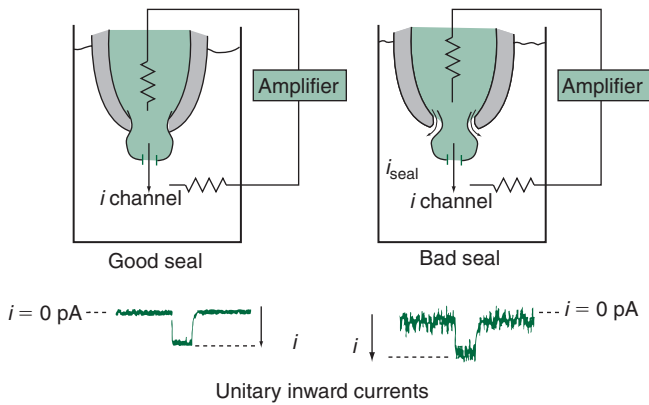


FIGURE A4.7 Good and bad seals.  
From *The Axon Guide*, Axon Instruments Inc., 1993.

no current can flow through the seal. This is important because if a fraction of the current passing through the membrane patch leaks out through the seal, it is not measured by the electrode.

- It augments the signal-to-noise ratio since thermal movement of the charges through a bad seal is a source of additional noise in the recording. A good seal thus enables the measurement of the current flowing through one single channel (unitary current) which is of the order of picoampères.

From the 'cell-attached' configuration (the last to be explained), one can obtain other recording configurations. In total, three of them are used to record unitary currents, and one (whole-cell) to record the current flowing through all the open channels of the whole cell membrane.

### Whole-cell configuration

This configuration is obtained from the cell-attached configuration. If a little suction is applied to the interior of the pipette, it may cause the rupture of the membrane patch under the pipette. Consequently, the patch pipette now records the activity of the whole cell membrane (minus the small ruptured patch of membrane). Rapidly, the intracellular solution equilibrates with that of the pipette, the volume of the latter being many times larger. This is especially true for inorganic ions.

This configuration enables the recording of the current flowing through the  $N$  channels open over the entire surface of the cell membrane. Under conditions where all the open channels are of the same type (with the opening of other channels being blocked by pharmacological agents or the voltage conditions), the total

current flowing through a population of identical channels can be recorded, such that at steady state:

$$I = Np_o i,$$

where  $N$  is the number of identical channels,  $p_o$  the probability that these channels are in the open state,  $Np_o$  the number of identical channels in the open state, and  $i$  the unitary current.

The advantages of this technique over the two-electrode voltage clamp technique are: (i) the recording under voltage clamp from cell bodies too small to be impaled with two electrodes and even one; and (ii) there is a certain control over the composition of the internal environment and a better signal-to-noise ratio. The limitation of this technique is the gradual loss of intracellular components (such as second messengers), which will cause the eventual disappearance of the responses dependent on those components.

### Perforated whole-cell configuration

This is a variation of the whole-cell configuration, and also allows the recording of current flowing through the  $N$  channels open in the whole membrane but avoids washout of the intracellular solution. This configuration is obtained by introducing into the recording pipette a molecule such as nystatin, amphotericin or gramicidin, which will form channels in the patch of membrane under the tip of the electrode. To record in this configuration, first the cell-attached configuration is obtained and then the experimenter waits for the nystatin channels (or amphotericin or gramicidin channels) to form without applying any suction to the electrode. The channels formed by these molecules are mainly permeable to monovalent ions and thus allow electrical access to the cell's interior. Since these channels are not permeant to molecules as large or larger than glucose, whole-cell recording can be performed without removing the intracellular environment. This is particularly useful when the modulation of ionic channels by second messengers is studied.

In order to evaluate this problem of 'washout', we can calculate the ratio between the cell body volume and the volume of solution at the very end of a pipette. For example, for a cell of 20  $\mu\text{m}$  diameter the volume is:  $(4/3)\pi(10 \times 10^{-6})^3 = 4 \times 10^{-15}$  litres. If we consider 1 mm of the tip of the pipette, it contains a volume of the solution approximately equal to  $10^{-13}$ l, which is 100 times larger than the volume of the cell body.

### Excised patch configurations

If one wants to record the unitary current  $i$  flowing through a single channel and to control simultaneously

the composition of the intracellular environment, the so-called excised or cell-free patch configurations have to be used. The *outside-out configuration* is obtained from the whole-cell configuration by gently pulling the pipette away from the cell. This causes the membrane patch to be torn away from the rest of the cell at the same time that its free ends reseal together. In this case the intracellular environment is that of the pipette, and the extracellular environment is that of the bath. This configuration is used when rapid changes of the extracellular solution are required to test the effects of different ions or pharmacological agents when applied to the extracellular side of the membrane.

The *inside-out configuration* is obtained from the cell-attached configuration by gently pulling the pipette away from the cell, lifting the tip of the pipette from the bath in the air and putting it back into the solution (interface of air-liquid). In this case, the intracellular environment is that of the bath and the extracellular one is that of the pipette (the pipette is filled with a pseudo-extracellular solution). This configuration is used when rapid changes in the composition of the intracellular environment are necessary to test, for example, the effects of different ions, second messengers and pharmacological agents in that environment.

#### Cell-attached configuration

The intracellular environment is that of the cell itself, and the extracellular environment of the recorded membrane patch is the pipette solution. This configuration enables the recording of current flowing through the channel or channels present in the patch of membrane that is under the pipette and is electrically isolated from the rest of the cell. If one channel opens at a time, then the unitary current  $i$  flowing through that channel can be recorded. The recordings in cell-attached mode present two limitations: (i) the composition of the intracellular environment is not controlled; and (ii) the value of the membrane potential is not known and can only be estimated.

Let us assume that the voltage in the interior of the patch pipette is maintained at a known value  $V_p$  ( $p$  = pipette). Since the voltage across the membrane patch is  $V_m = V_i - V_e = V_i - V_p$ , it will not be known unless  $V_i$ , the voltage at the internal side of the membrane, is also known.  $V_i$  cannot be measured directly. One way to estimate this value is to measure the resting potential of several identical cells under similar conditions (with intracellular or whole-cell recordings), and to calculate an average  $V_i$  from the individual values. Sometimes, however,  $V_i$  can be measured when the cell is large enough to allow a two-electrode voltage clamp recording to be made simultaneously

with the patch clamp recording (with a *Xenopus* oocyte, for example). Another method consists of replacing the extracellular medium with isotonic  $K^+$  (120–150 mM). The membrane potential under these conditions will be close to 0 mV.

To leave the intracellular composition intact while recording the activity of a single channel is particularly useful for studies of the modulation of an ionic channel by second messengers.

### A4.3.2 Principles of the patch clamp recording technique

In the patch clamp technique, as in all voltage clamp techniques, the membrane potential is held constant (i.e. clamped) while the current flowing through a single open channel or many open channels ( $Np_o$ ) is measured (**Figure A4.8**). In the patch clamp technique only one micropipette is used full time for both voltage clamping and current recording. How at the same time via the same pipette can the voltage of the membrane be controlled and the current flowing through the membrane be measured?

When an operational amplifier A1 is connected as shown in **Figure A4.8a** with a high megohm resistor  $R_f$  ( $f$  = feedback), a current-to-voltage converter is obtained. The patch pipette is connected to the negative input and the command voltage ( $V_{cmd}$ ) to the positive one. The resistor  $R_f$  can have two values:  $R_f = 1\text{ G}\Omega$  in the whole-cell configuration and  $10\text{ G}\Omega$  in the excised patch configurations.

#### How the membrane is clamped at a voltage equal to $V_{cmd}$

$R_p$  represents the electrode resistance and  $R_m$  the membrane input resistance (**Figure A4.8a**). Suppose that the membrane potential is first clamped to  $-80\text{ mV}$  ( $V_{cmd} = -80\text{ mV}$ ), then a voltage step to  $-20\text{ mV}$  is applied for 100 ms ( $V_{cmd} = -20\text{ mV}$  for 100 ms). The membrane potential ( $V_m$ ) has to be clamped quickly to  $-20\text{ mV}$  ( $V_m = V_{cmd} = -20\text{ mV}$ ) whatever happens to the channels in the membrane (they open or close). The operational amplifier A1 is able to minimize the voltage difference between two inputs to a very small value ( $0.1\text{ }\mu\text{V}$  or so). A1 compares the value of  $V_{cmd}$  (entry +) to that of  $V_m$  (entry -). It then sends a voltage output ( $V_o$ ) in order to obtain  $V_m = V_{cmd} = -20\text{ mV}$  (**Figure A4.8b**).

What is this value of  $V_o$ ? Suppose that at the time  $t$  of its peak the  $\text{Na}^+$  current evoked by the voltage step to  $-20\text{ mV}$  is  $I_{\text{Na}} = 1\text{ nA}$ .  $V_o$  will force a current  $I = -1\text{ nA}$  to flow through  $R_f = 10^9\text{ }\Omega$  in order to clamp the membrane potential:  $V_o = R_f I = 10^9 \times 10^{-9} = 1\text{ V}$ . It is said that  $V_o = 1\text{ V/nA}$  or  $1\text{ mV/pA}$ .

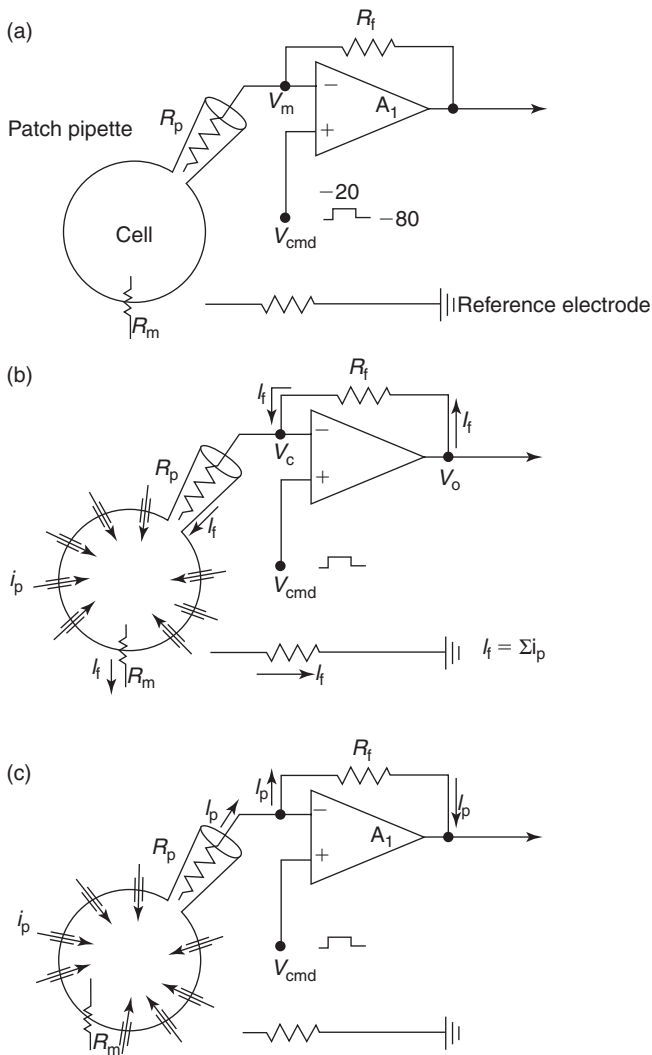


FIGURE A4.8 Example of a patch clamp recording in the whole-cell configuration.

(a) The amplifier compares  $V_m$  to the new  $V_{\text{cmd}} = -20\text{ mV}$ . (b) The amplifier sends  $V_o$  so that  $V_m = V_{\text{cmd}} = -20\text{ mV}$ . Owing to the depolarization to  $-20\text{ mV}$ , the  $\text{Na}^+$  channels open and unitary inward currents  $i_p$  flow through the  $N$  open channels ( $Ni_p = I_p$ ). (c) The whole-cell current  $I_p$  flows through the circuit and is measured as a voltage change.

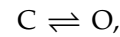
The limits of  $V_o$  in patch clamp amplifiers are  $+15\text{ V}$  and  $-15\text{ V}$ . This means that  $V_o$  cannot be bigger than these values, which is largely compatible with biological experiments where currents through the membrane do not exceed  $15\text{ nA}$ .

The amplifier  $A_1$  compares  $V_m$  with  $V_{\text{cmd}}$  and sends  $V_o$  at a very high speed. This speed has to be very high in order to correct  $V_m$  according to  $V_{\text{cmd}}$  very quickly. The ideal clamp is obtained at the output of the circuit via  $R_f$  (black dot  $V_c$  on the scheme of Figure A4.8b). As in the voltage clamp technique, a capacitive current is present at the beginning and at the end of the voltage step on the current trace and a leak current during the step, but they are not re-explained here.

### A4.3.3 The unitary current $i$ is a rectangular step of current (see Figures 4.8a and c)

We record, for example, in the outside-out patch clamp configuration to activity of a single voltage sensitive  $\text{Na}^+$  channel. When a positive membrane potential step is applied to depolarize the patch of membrane from  $-90\text{ mV}$  to  $-40\text{ mV}$ , an inward current  $i_{\text{Na}}$  flowing through the open  $\text{Na}^+$  channel is recorded (inward current means a current that flows across the membrane from the outside to inside). By convention, inward currents are represented as downward deflections and outward currents as upward deflections.

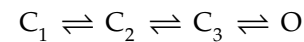
The membrane depolarization causes activation of the voltage-dependent  $\text{Na}^+$  channel, and induces its transition from the closed (C) state (or conformation) to the open (O) state, a transition symbolized by:



where C is the closed state of the channel (at  $-90\text{ mV}$ ) and O is the open state of the channel (at  $-40\text{ mV}$ ).

While the channel is in the O conformation (at  $-40\text{ mV}$ ),  $\text{Na}^+$  ions flow through the channel and an inward current caused by the net influx of  $\text{Na}^+$  ions is recorded. This current reaches its maximum value very rapidly. Thus, the maximal net ion flux is established almost instantaneously given the timescale of the recording (of the order of microseconds). The development of the inward current thus appears as a vertical downward deflection.

A delay between the onset of the voltage step and the onset of the current  $i$  is observed. This delay has a duration that varies from one depolarizing test pulse to another and also according to the channel under study. This delay is due to the conformational change or changes of the protein. In fact, such changes previous to opening can be multiple:



Notice that the opening delay does not correspond to the intrinsic duration of the process of conformational change, which is extremely short. It corresponds to the statistical nature of the equilibrium between the 2, 3,  $N$  closed and open conformations. The opening delay therefore depends on the time spent in each of the different closed states ( $C_1, C_2, C_3$ ).

The return of the current value to zero corresponds to the closing of the channel. This closure is the result of the transition of the channel protein from the open state (O) to a state in which the channel no longer conducts (state in which the aqueous pore is closed). It can be either a closed state (C), an inactivated state (I) or a desensitized state (D). In the case of the  $\text{Na}^+$  channel,



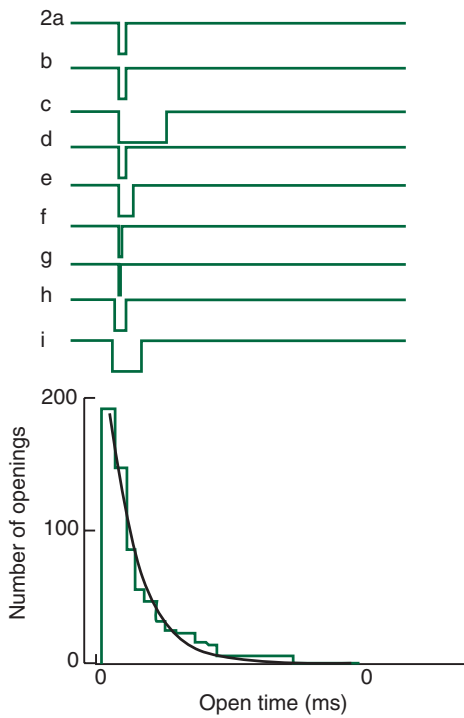


FIGURE A4.10 Determination of the mean open time of a channel.

Trial 2 of Figure A4.9 is selected and all the openings are aligned at time 0.  $\tau_o = 1.2$  ms.

#### Why does the distribution of $t_o$ decrease?

The histogram is constructed as follows. At time  $t = 0$ , all the channels are open (the delay of opening is ignored, all the openings are aligned at time 0; **Figure A4.10**). As time  $t$  increases, the number of channels that remain open can only decrease since channels progressively close. This can also be expressed as follows: the longer the observation time, the lower the probability that the channel is still in the open state. Or, alternatively, the longer the observation time, the closer the probability will be to 1 that the channel will shut (1 is the maximum value used to express a probability). It is not a Gaussian curve because the delay of opening is ignored and all the openings begin at  $t = 0$ .

#### Why is the decremting distribution of $t_o$ exponential?

A channel open at  $t = 0$  has a probability of closing at  $t + \Delta t$ . It has the same probability of closing if it is still

open at the beginning of any subsequent observation interval  $\Delta t$ . This type of probability is described mathematically as an exponential function of the observation time. Thus, when the openings of a homogeneous population of channels are studied, the decrease in the number of events is described by a single exponential.

#### Experimental determination of $\tau_o$ , the mean open time of a channel

The mean open time  $\tau_o$  is the time during which a channel has the highest probability of being in the open state: it corresponds to the sum of all the values that  $t_o$  may take, weighted by their corresponding probability values. This value is easy to calculate if the distribution is described by a single exponential. In order to verify that the histogram is actually described by a single exponential, one has to first build the histogram by plotting the number of times a value of  $t_o$  is observed as a function of  $t_o$ ; i.e. number of events =  $f(t_o)$ .

The exponential that describes the histogram has the form  $y = y_0 e^{-t/\tau_o}$ , where  $y$  is the number of events observed at each time  $t$ . This curve will be linear on semi-logarithmic coordinates if it is described by a single exponential. The slope can be measured with a regression analysis. It corresponds to the mean open time  $\tau_o$  of the channel.  $\tau_o$  is the value of  $t_o$  for a number of events equal to  $1/e$ . It is the 'expected value' of  $t_o$ . The expected value of  $t_o$  is the sum of all the values of  $t_o$  weighted to their corresponding probabilities.

In the case of the conformational changes  $C \rightleftharpoons O$ , the value of  $\tau_o$  provides an estimate of the closure rate constant  $\alpha$ , because at steady state  $\tau_o = 1/\alpha$ . For example, from the open time histogram of the nicotinic receptor channel, we can determine its mean open time  $\tau_o$ . Knowing that in conditions where the desensitization of the channel is negligible  $\tau_o = 1/\alpha$ , we can calculate from  $\tau_o$  the closing rate constant of the channel. If  $\tau_o = 1.1$  ms,  $\alpha = 900 \text{ s}^{-1}$ . The channel closes 900 times for each second spent in the open state. In other words there is an average of 900 transitions of the channel to the closed state for each second spent in the open state.